

## Synthesis and Characterization of NUC-7738, an Aryloxy Phosphoramidate of 3'-Deoxyadenosine, as a Potential Anticancer Agent

Michaela Serpi,\* Valentina Ferrari, Christopher McGuigan, Essam Ghazaly, and Chris Pepper

Cite This: *J. Med. Chem.* 2022, 65, 15789–15804

Read Online

ACCESS |



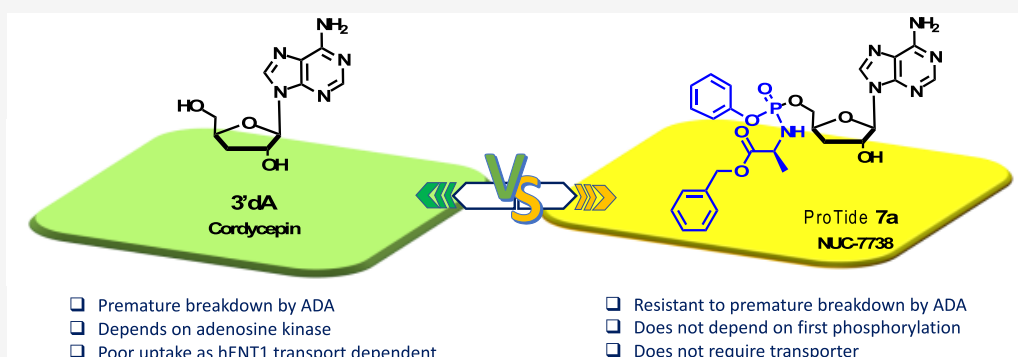
Metrics &amp; More



Article Recommendations



Supporting Information



**ABSTRACT:** 3'-Deoxyadenosine (3'-dA, Cordycepin, **1**) is a nucleoside analogue with anticancer properties, but its clinical development has been hampered due to its deactivation by adenosine deaminase (ADA) and poor cellular uptake due to low expression of the human equilibrative transporter (hENT1). Here, we describe the synthesis and characterization of NUC-7738 (**7a**), a 5'-aryloxy phosphoramidate prodrug of 3'-dA. We show *in vitro* evidence that **7a** is an effective anticancer drug in a panel of solid and hematological cancer cell lines, showing its preferential cytotoxic effects on leukemic stem cells. We found that unlike 3'-dA, the activity of **7a** was independent of hENT1 and kinase activity. Furthermore, it was resistant to ADA metabolic deactivation. Consistent with these findings, **7a** showed increased levels of intracellular 3'-deoxyadenosine triphosphate (3'-dATP), the active metabolite. Mechanistically, levels of intracellular 3'-dATP were strongly associated with *in vitro* potency. NUC-7738 is now in Phase II, dose-escalation study in patients with advanced solid tumors.

## INTRODUCTION

3'-Deoxyadenosine (3'-dA, cordycepin, **1**) (Figure 1) is the main bioactive component isolated from the fermented broth of *Cordyceps militaris*, which is a medicinal parasitic fungus. This fungus has been used in traditional Chinese medicine for over 300 years as a treatment for inflammatory diseases and cancer.<sup>1–5</sup> 3'-dA is a nucleoside analogue similar in structure to adenosine but lacking the 3'-hydroxyl group on the ribose moiety, and it has been proposed as an anticancer drug due to its numerous biological and pharmacological actions including inhibition of cell proliferation, induction of apoptosis, antimetastatic effect, and immune system activation.<sup>6</sup> The mechanism of its antitumor activity is not well understood, but 3'-dA has been shown to regulate several signaling pathways associated with tumor growth and metastasis.<sup>7,8</sup> 3'-dA is thought to enter cells via the human equilibrative nucleoside transporters (hENT1),<sup>9</sup> and to be phosphorylated by adenosine kinase (AK) to 3'-deoxyadenosine monophosphate (3'-dAMP). 3'-dAMP is phosphorylated twice to the active metabolite 3'-deoxyadenosine triphosphate (3'-dATP) by the

combined actions of adenosine monophosphate kinase (AMPK) and nucleoside diphosphate kinases (NDPK) (Figure 1).<sup>10</sup> 3'-dA is also subject to metabolism by adenosine deaminase (ADA), which rapidly metabolizes it to the inactive 3'-deoxyinosine (3'-dIno, Figure 1).<sup>11–13</sup> Due to the structural similarity with adenosine triphosphate (ATP), 3'-dATP can provoke termination of RNA elongation by incorporating into the site where nucleic acids are supposed to incorporate.<sup>10</sup> 3'-dATP may also compete with ATP for binding to the epidermal growth factor receptor (EGFR) binding site. It has been suggested that 3'-dATP blocks the phosphorylation of EGFR and therefore interferes with the caspase and GSK-3 $\beta$  mediated pathways.<sup>14</sup> 3'-dATP has also been shown to inhibit

Received: August 17, 2022

Published: November 23, 2022



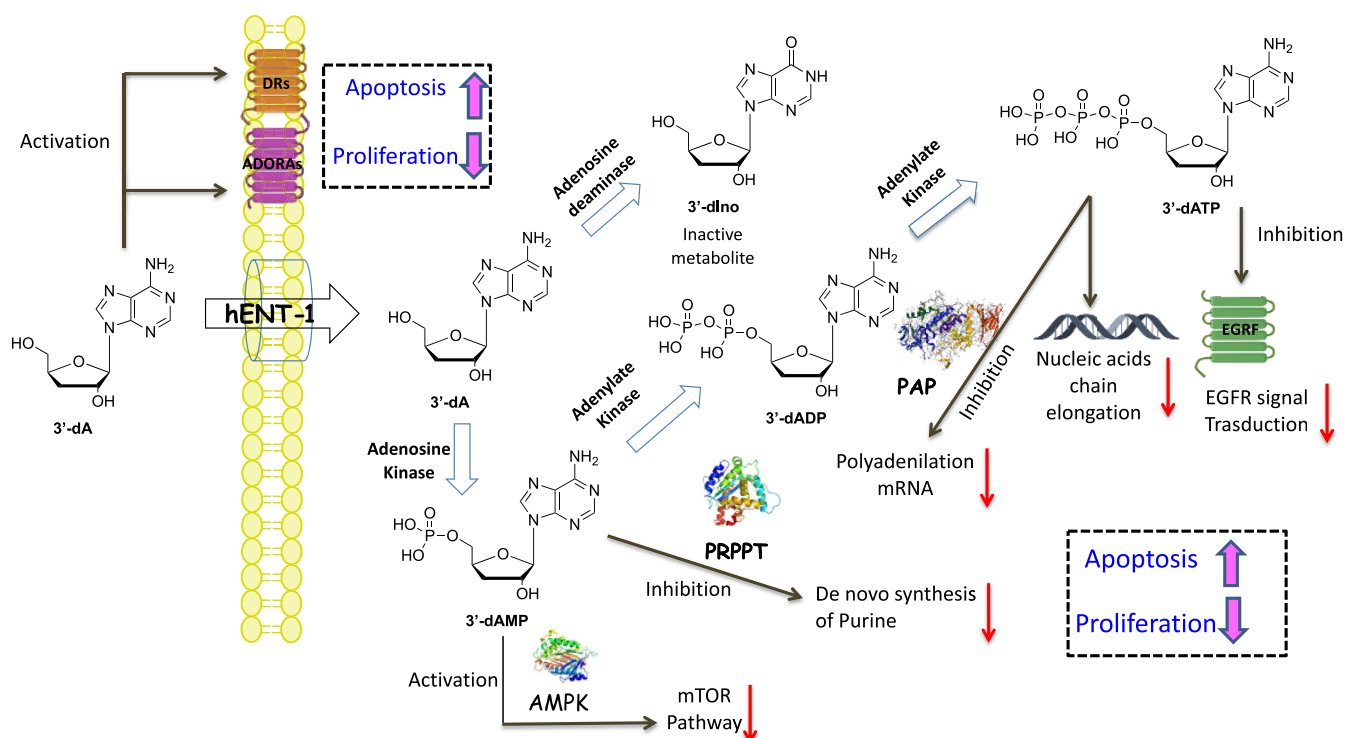


**Figure 1.** Transport (gray arrow), metabolism (blue arrows), and mode of action (black arrows) of 3'-dA and its metabolites. 3'-dA enters the cell via the human equilibrative nucleoside transporters (hENT1), then it is phosphorylated by adenosine kinase (AK) to 3'-deoxyadenosine monophosphate (3'-dAMP), which in turn is phosphorylated twice to 3'-deoxyadenosine triphosphate (3'-dATP) by the combined actions of adenosine monophosphate kinase (AMPK) and nucleoside diphosphate kinases (NDPK). 3'-dA is metabolized to 3'-deoxyinosine (3'-dIIno) by adenosine deaminase (ADA). Mode of action: 3'-dATP provokes termination of RNA elongation and inhibits polyadenylate polymerase (PAP). It also interrupts EGFR signal transduction. 3'-dAMP inhibits the activity of phosphoribosyl-pyrophosphate aminotransferase (PRPPT) and activates AMPK. 3'-dA mediates apoptotic signaling via adenosine (ADORAs) and death receptors (DRs) to inhibit lung cancer cell proliferation and induce apoptosis. All of these activities lead to apoptosis and inhibition of cell proliferation.

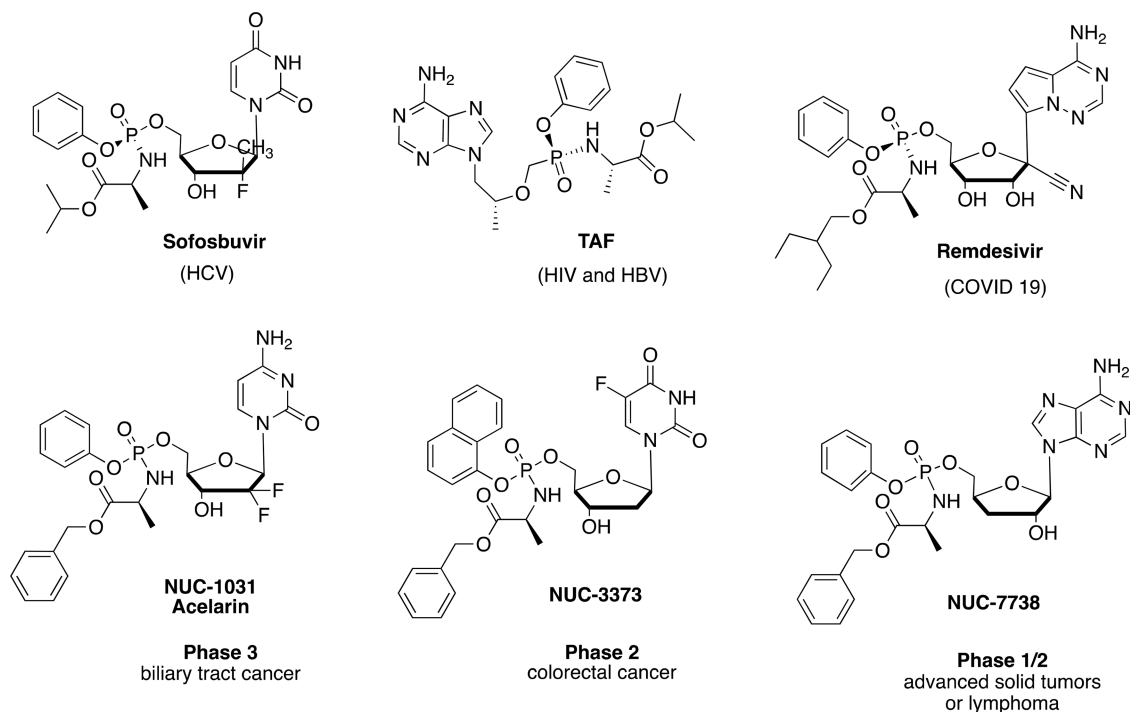
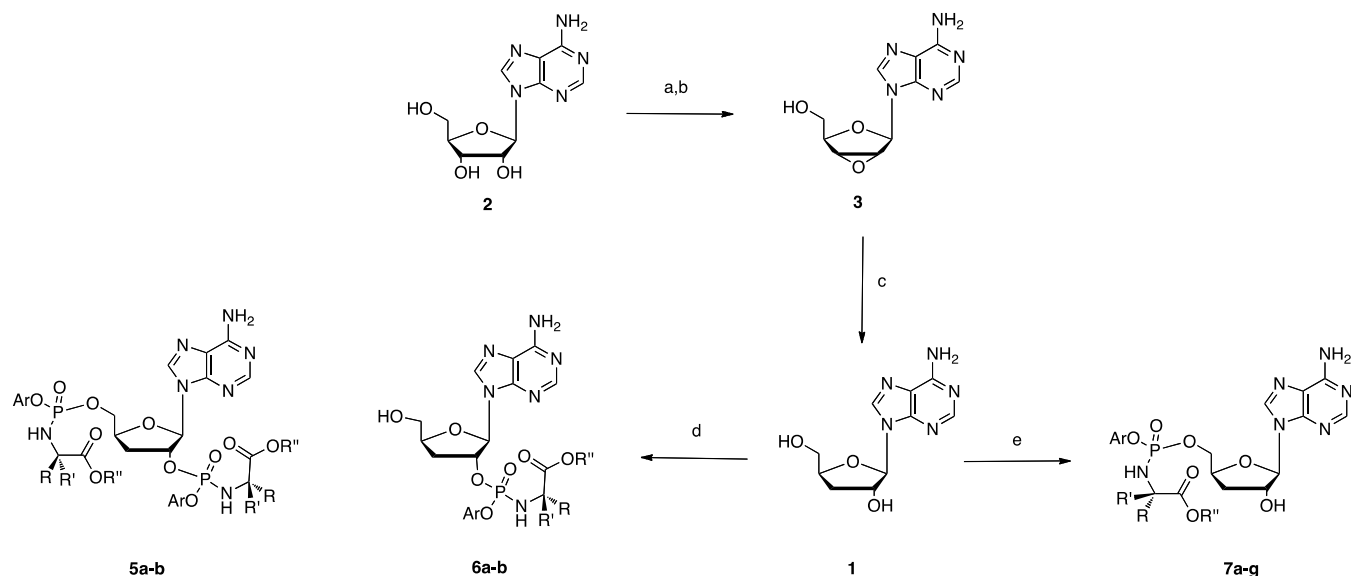


**Figure 2.** FDA-approved and clinical candidate ProTides.

**Scheme 1. Reagents and Conditions:** (a)  $\alpha$ -AIBr (4 equiv),  $\text{H}_2\text{O}/\text{CH}_3\text{CN}$ , rt, 1h; (b) Amberlite (IRN78) (8 mL/mmol),  $\text{CH}_3\text{OH}$ , rt, 16 h, 98%; (c)  $\text{LiEt}_3\text{BH}$  DMSO (4 mL/mmol) tetrahydrofuran (THF, 10 mL/mmol),  $0^\circ\text{C}$  to rt, 16 h, 95%; (d) 1 M  $t\text{BuMgCl}$  in THF (1.1 equiv), 4a–b (3 equiv), anhydrous THF, rt, 16 h, 5–35% (e) NMI (5 equiv), 4a–f (3 equiv), anhydrous THF, rt, 16 h, 6–28%



polyadenylate polymerase (PAP), an enzyme responsible for the polyadenylation of mRNA.<sup>10</sup> Furthermore, 3'-dAMP inhibits the activity of phosphoribosyl-pyrophosphate aminotransferase (PRPPT), which impedes *de novo* purine synthesis,<sup>15</sup> and activates AMPK downregulating mTORC1 function and HIF-1 $\alpha$  expression in tumor cells.<sup>16</sup> 3'-dA has been suggested to mediate apoptotic signaling via adenosine receptors (ADORAs) in glioma,<sup>17</sup> bladder,<sup>18</sup> melanoma, and lung carcinoma<sup>19</sup> cell lines and via death receptors (DRs) in colon and prostate cancer cell lines.<sup>20,21</sup> Despite all of these activities and the potent anticancer activity observed in *in vitro* studies, 3'-dA has not been successfully developed or approved as a chemotherapeutic agent. 3'-dA efficacy is severely limited by its rapid metabolite into an inactive metabolite by ADA. Downregulation of hENT1 transporter and lack of expression of kinase enzymes, which have been found after drug resistance develops in multiple cancers,<sup>22</sup> are also responsible for the reduced efficacy of 3'-dA due to its poor cellular uptake and activation.<sup>13,23</sup> In response to some of these limitations, 3'-dA entered clinical trials in combination with the ADA inhibitor, pentostatin. Two phase I clinical studies in patients with refractory acute lymphocytic or chronic myelogenous leukemia<sup>24</sup> and phase I/II studies in patients with refractory TdT-positive leukemia<sup>25</sup> have been reported; however, it remains unclear if either of these studies completed recruitment or generated results. It is worthy of note that given the critical role that ADA plays in several human metabolic pathways, treatment strategies that require the co-administration of an ADA inhibitor may restrict the clinical development of 3'-dA.

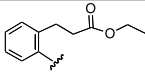
Exploiting phosphoramidate chemistry, nucleoside analogues have been converted into activated nucleotide analogues with the addition at the 5' position of a phosphate group protected by specific combinations of aryl and amino acid ester moieties.<sup>26</sup> These prodrugs are designed to deliver the active metabolite of the parental nucleoside directly into cells, bypassing the resistance mechanisms associated with transportation, activation, and breakdown. The ProTide

approach has been particularly successfully applied to antiviral nucleosides<sup>27</sup> as evidenced by the development and approval of the currently marketed drugs Sofosbuvir<sup>28</sup> and Tenofovir Alafenamide (TAF),<sup>29</sup> respectively, approved for the treatment of HCV and HIV, and Remdesivir, authorized for temporary use as a COVID-19 treatment (Figure 2).<sup>30</sup> In the oncology setting, three clinical candidates Acelarin,<sup>31,32</sup> NUC-3373,<sup>33</sup> and NUC-7738<sup>34</sup> are currently under clinical evaluation as anticancer agents (Figure 2).<sup>35–41</sup> Here, we report the design, synthesis, and biological evaluation of a family of phosphoramidates of 3'-dA, which were designed to bypass the premature breakdown by ADA of 3'-dA and its hENT-1 and kinase dependence. This study has led to the selection of NUC-7738 as a clinical candidate, now in phase 1/2 clinical evaluation for the treatment of advanced solid tumors or lymphomas.<sup>37,41</sup>

## RESULTS AND DISCUSSION

**Chemistry.** In the past, 3'-dA was mainly obtained by extraction from *Cordyceps militaris*. However, due to the low amount of 3'-dA in the fungus (2–3 mg/kg), chemical synthesis has slowly replaced extraction as a means of producing it. Many different strategies for the synthesis of 3'-dA starting either from non-nucleoside<sup>42–45</sup> or nucleoside starting materials<sup>46–50</sup> are reported in the literature. After careful consideration, we decided to follow the synthetic route developed by Meier et al. (Scheme 1).<sup>48</sup> Briefly, adenosine (2) was first converted into 9-(2,3-anhydro- $\beta$ -D-ribofuranosyl)-adenine (3) with a 98% yield. Then, metal hydride-mediated reductive opening of the epoxide ring in 3 afforded cordycepin (1) as the only regioisomer with a 95% yield. To generate phosphoramidates of 3'-dA, we first applied the procedure involving the use of *t*-butyl magnesium chloride ( $t\text{BuMgCl}$ ) as a base and a phosphochloridate as a phosphorylating reagent.<sup>51</sup> However, the reaction of phosphochloridates 4a–b with 1 in these conditions led to the formation of two products, which, through careful analysis of two-dimensional NMR spectra, were identified as the 2',5'-*O*-bis phosphoramidates 5a–b and

Table 1. Chemical Composition and Yield of the Synthesized 3'-dA ProTides

Comp.	Isomer	Ar	R	R'	R''	Yield (%)
5a	2',5'-bis OP	Ph	CH <sub>3</sub>	H	CH <sub>2</sub> Ph	11
5b	2',5'-bis OP	1-NaPht	CH <sub>3</sub>	H	CH <sub>2</sub> Ph	5
6a	2'-OP	1-Napht	CH <sub>3</sub>	H	CH(CH <sub>3</sub> ) <sub>2</sub>	35
6b	2'-OP	1-Napht	CH <sub>3</sub>	H	CH <sub>2</sub> Ph	11
7a	5'-OP	Ph	CH <sub>3</sub>	H	CH <sub>2</sub> Ph	28
7b	5'-OP	1-Napht	CH <sub>3</sub>	H	CH <sub>2</sub> Ph	12
7c	5'-OP	Ph	H	H	CH <sub>2</sub> Ph	19
7d	5'-OP	1-Napht	CH <sub>2</sub> CH(CH <sub>3</sub> ) <sub>2</sub>	H	(CH <sub>2</sub> ) <sub>4</sub> CH <sub>3</sub>	22
7e	5'-OP		CH <sub>3</sub>	H	CH <sub>2</sub> Ph	18
7f	5'-OP	1-Napht	CH <sub>3</sub>	CH <sub>3</sub>	CH <sub>3</sub>	6

2'-O-phosphoramidates **6a–b**. On the contrary, when the coupling reaction was performed with *N*-methyl imidazole (NMI),<sup>51</sup> 5'-phosphoramidates **7a–g** were synthesized as the major products in moderate yields, together with the corresponding 2',5'-O-bis phosphoramidates as side products (not isolated). The choice of promoieties was based on our previous findings (Table 1).<sup>26</sup>

Differences in the stereochemistry of drugs have often led to compounds with different activities, toxicologies, and metabolisms, hence the preference for using single isomers as clinical agents. In the case of ProTides, crucial examples are the marketed drugs sofosbuvir and TAF, whose *Sp* isomers were 18-fold and 10-fold more active than the *Rp* isomers, respectively.<sup>52,53</sup> Other examples of ProTides, whose separated diastereoisomers showed different activity profiles,<sup>54</sup> rates of enzymatic activation<sup>33,55</sup> or differential transport through intestinal absorption cell models are also reported in the literature.<sup>56</sup> Although reported, diastereoisomeric separation<sup>57,58</sup> of ProTides or their preparation<sup>59–61</sup> as single diastereoisomers are not always straightforward. Our attempts to separate the diastereoisomers of ProTides **7a** (NUC-7738) (selected compound from this study) via direct phase silica gel column chromatography were ineffective due to the very close retention times of both isomers on silica. Attempts to separate 3'-dA phosphoramidate diastereoisomers bearing different silane protecting groups at the 2' position, as previously reported for ProTides of different nucleosides,<sup>62</sup> were also unsuccessful. This protection strategy, although ineffective for the separation of the two diastereoisomers, proved to be a more efficient way to prepare **7a**, with an overall yield of 42%.<sup>34</sup> Separation of the isomers of **7a** was instead achieved via reversed-phase high-performance liquid chromatography (Figure S1) or Biotage Isolera using isocratic elution with 55% methanol in water. Structural elucidation studies were subsequently performed on **7a** slow-eluting isomer, obtained from reversed-phase separation. Single-crystal analysis from crystals obtained from ethyl acetate confirmed the presence of a 1:1 solvated species and the absolute configuration of this isomer was determined to be *S* around the phosphorus chiral center. The asymmetric unit is shown in Figure 3.

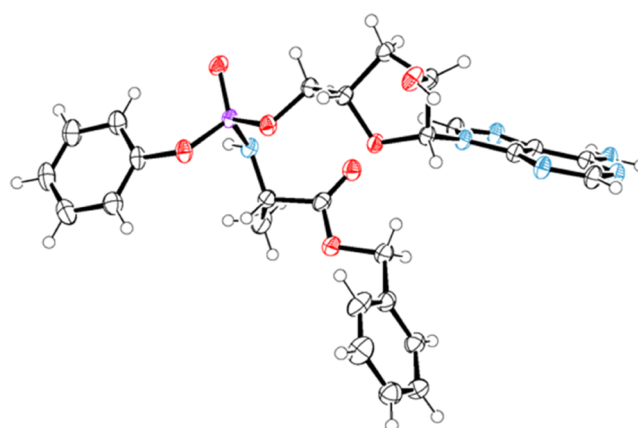
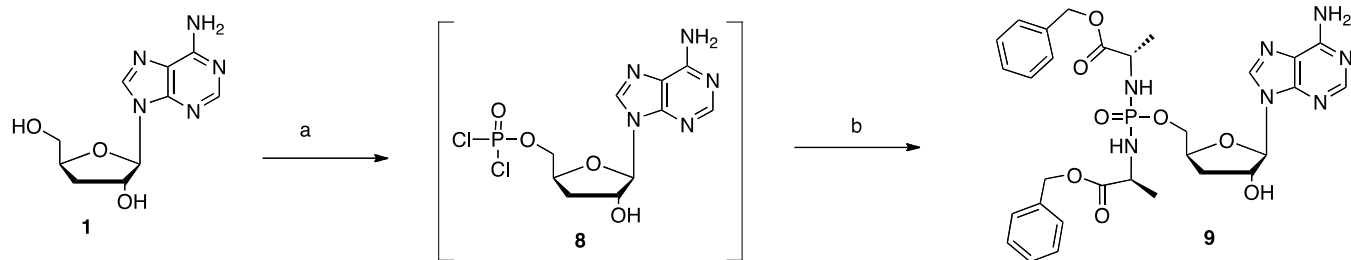


Figure 3. ORTEP view of the **7a-Sp** molecule crystal structure from the ethyl acetate solvate. All nonhydrogen atoms are shown with thermal ellipsoids set at the 50% probability level. Color code: carbon = gray, hydrogen = white, oxygen = red, and phosphorous = purple.

Although less investigated than the ProTides, the phosphorodiamidates in which two identical amino acid esters are introduced onto the monophosphate moiety through a P–N bond to mask the negative charges have been reported as valid alternatives for the delivery of nucleoside monophosphates into a cell.<sup>63,64</sup> Due to their symmetric structure, phosphorodiamidates offer the advantage of not having a chiral phosphorus compared to the aryloxy monoamidate analogues. As previously reported for other nucleosides, we used a slightly modified Yoshikawa procedure applied to 3'-dA to obtain bis benzyloxy-L-alanyl phosphorodiamidate **9** from unprotected 3'-dA with a 49% yield (Scheme 2).<sup>65</sup>

**In Vitro Cytotoxic Activity.** All of the synthesized compounds and the parent nucleosides were tested against a wide panel of cancer cell lines (Tables 2–4 and Table S1). In the majority of cell lines investigated, 3'-dA did not show potent anticancer activity, as evidenced by the high LC<sub>50</sub> values (the concentration required to kill 50% of the cells in culture) and the inability to reach 100% cell death. The exceptions were the mantle cell lymphoma cell line, Z138 (LC<sub>50</sub> = 12.15 μM), and the erythroleukemia cell line, HEL92.1.7 (LC<sub>50</sub> = 68.9

**Scheme 2. Reagents and Conditions:** (a) POCl<sub>3</sub> (1 equiv), TMP, 0 °C to rt, 4 h. (b) L-AlaOBn·HCl (5 equiv), *N,N*-diisopropylethylamine (DIPEA, 10 equiv), CH<sub>2</sub>Cl<sub>2</sub>, 0 °C to rt, 16 h, 49%



**Table 2. Cytotoxic Activity of 3'-dA and Compounds 7a–f, 9<sup>a</sup>**

comp	CCRF-CEM		HL-60		KG-1		MOLT-4		K562		MV4-11		THP-1	
	LC <sub>50</sub>	MI <sub>%</sub>	LC <sub>50</sub>	MI <sub>%</sub>	LC <sub>50</sub>	LC <sub>50</sub>	LC <sub>50</sub>	MI <sub>%</sub>						
3'-dA	>198	12	76.84	88	70.82	78	151.92	52	59.31	88	>198	1	>198	-3
7a	2.36	100	17.78	97	17.36	92	0.51	98	6.1	92	2.1	99	65.45	74
Rp-7a	1.86	97	8.7	100	14.0	90	0.57	98	2.60	95	0.98	100	35.0	91
Sp-7a	2.04	97	11	92	18.0	90	0.43	98	3.0	96	1.03	100	66.0	69
7b	1.17	100	6.37	100	11.03	100	0.32	100	4.93	97	1.48	99	46.47	99
7c	14.93	94	45.23	82	136.56	65	3.55	93	15.42	92	-	-	-	-
7d	4.72	100	8.9	100	12.02	99	1.46	100	11.7	99	8.78	106	68.91	99
7e	40.09	90	78.51	74	102.14	69	12.62	97	174.71	61	3.27	100	36.66	100
7f	4.92	99	24.08	98	>198	29	1.4	100	10.69	91	8.71	101	>198	43
9	7.03	100	16.53	100	34.13	98	3.52	100	24.34	97	-	-	-	-
PTX	0.003	95	0.004	96	0.07	89	0.002	97	0.008	94	0.01	99	0.03	72

<sup>a</sup>Cytotoxicity data reported as  $\mu$ M LC<sub>50</sub> values (concentration of drug causing 50% cell death) and MI% values (maximum inhibitory effect of the drug at the range of concentrations considered). PTX: paclitaxel (control); (-) not tested.

**Table 3. Cytotoxic Activity of 3'-dA and Compounds 7a,b, d–f<sup>a</sup>**

comp	HEL92.1.7		NCI-H929		RPMI-8226		Jurkat		Z138		RL		HS445	
	LC <sub>50</sub>	MI <sub>%</sub>												
3'-dA	68.9	88	>198	24	>198	1	>198	20	12.15	95	>198	17	>198	2
7a	8.07	100	6.07	100	14.72	96	1.44	100	26.97	95	3	93	30.53	98
Rp-7a	11.0	98	19.0	97	25.0	90.8	2.82	97	-	-	4.0	96.8	42.0	99
Sp-7a	11.0	100	16.0	94	19.0	86.8	2.29	90	-	-	2.64	92.6	67.0	75
7b	2.94	98	3.38	99	9.48	102	0.9	100	6.32	100	1.68	96	10.18	96
7d	4.23	99	7.21	104	24.06	103	7.15	100	5.65	100	11.61	100	39.53	102
7e	14.49	99	7.57	100	31.05	106	4.75	100	68.18	76	7.26	90	42.73	92
7f	15.42	101	16.11	98	46.7	89	7.01	95	43.84	93	13.54	88	54.98	85
PTX	0.02	83	0.003	82	0.003	91	0.005	97	0.002	99	0.003	83	0.01	74

<sup>a</sup>Cytotoxicity data reported as  $\mu$ M LC<sub>50</sub> values (concentration of drug causing 50% cell death) and MI% values (maximum inhibitory effect of the drug at the range of concentrations considered). PTX: paclitaxel (control); (-) not tested.

$\mu$ M). No rationale for these dichotomous results could be found in the literature, but it might be speculated that these cell lines have lower constitutive levels of ADA, which could enhance the activity of 3'-dA.

As is evidenced by the results, the 3'-dA prodrugs conferred an advantage over the parental nucleoside in terms of cytotoxicity in almost all cell lines. Among all of the prodrugs, the 5'-phosphoramidates (7a–f) were the most active in hematological tumor cell lines, reported in Tables 2 and 3, and their results against solid tumor cell lines are shown in Table 4 (see Table S1 in the Supporting Information for results of the 2',5'-O-bis phosphoramidates 5a,b and the 2'-phosphoramidates 6a,b). Among the 5' derivatives, 7a and 7b emerged as the most active in most of the cell lines tested. The *L*-leucine pentyl derivative 7d also showed potent anticancer activity but was always 1- to 3-fold less active compared to 7a and 7b.

Replacing the amino acid portion with glycine, as in 7c or dimethylglycine 7f, led to a decrease in anticancer activity, especially in the case of compound 7f, which also contained a methyl ester instead of a benzyl ester. The introduction of an ethyl propanoic ester side chain in the *ortho* position of the phenyl ring generated compound 7e, which had similar or higher LC<sub>50</sub> values compared to 7a and 7b. This side chain was strategically introduced, as upon activation, compound 7e releases hydroxyphenyl propanoic acid, which is a known nontoxic metabolite of dihydrocoumarin, a common flavoring agent widely used in food and cosmetics.<sup>66</sup>

ProTides 7a and 7b were approximately 200-fold more active than 3'-dA and in the Jurkat cell line (acute T-cell leukemia) with LC<sub>50</sub> values of 1.44 and 0.9  $\mu$ M, respectively. Their cytotoxic activities in solid tumor cell lines were lower compared to hematological tumors, but again, ProTides 7a and

Table 4. Cytotoxic Activity of 3'-dA and Compounds 7a–f, 9<sup>a</sup>

comp	HepG2		MCF-7		BxPC-3		HT29		MIA PaCa-2		SW620	
	LC <sub>50</sub>	MI <sub>%</sub>										
3'-dA	142.47	66	34.23	78	>198	22	>198	44	>198	35	>198	10
7a	18.73	76	3.07	94	23.59	81	13.42	93	6.85	96	24.94	85
Sp-7a	57.0	73	5.87	94	99.0	73	25.0	95	18.0	94	35.0	87
Rp-7a	32.0	78	2.94	97	74.0	71	16.0	97	14.0	96	29.0	82
7b	11.53	95	1.39	99	13.36	90	7.52	98	3.73	98	11.41	93
7c	142.35	59	15.46	87	-	-	-	-	-	-	-	-
7d	9.53	99	2.48	100	65.46	99	16.06	99	14.69	106	35.48	100
7e	96.11	59	15.78	78	60.92	78	25.24	89	12.09	101	43.4	90
7f	70.22	84	9.10	99	76.18	71	37.94	76	17.55	91	56.48	74
9	156.87	55	12.97	97	-	-	-	-	-	-	-	-
PTX	#intersect	54	0.003	79	>0.5	42	0.004	75	0.002	87	0.02	96

<sup>a</sup>Cytotoxicity data reported as  $\mu\text{M}$  LC<sub>50</sub> values (concentration of drug causing 50% cell death) and MI% values (maximum inhibitory effect of the drug at the range of concentrations considered). PTX: paclitaxel (control); (-) not tested.

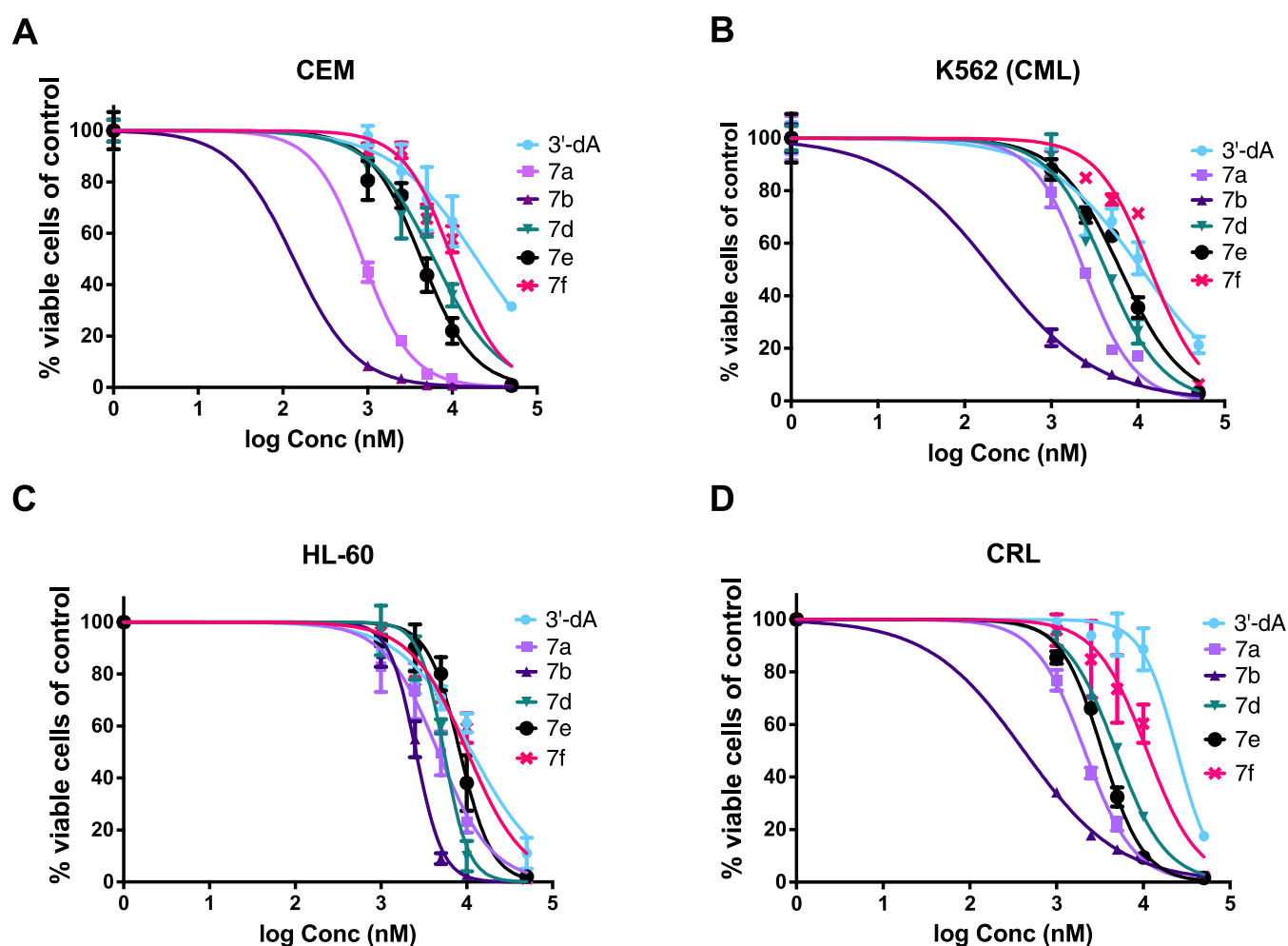
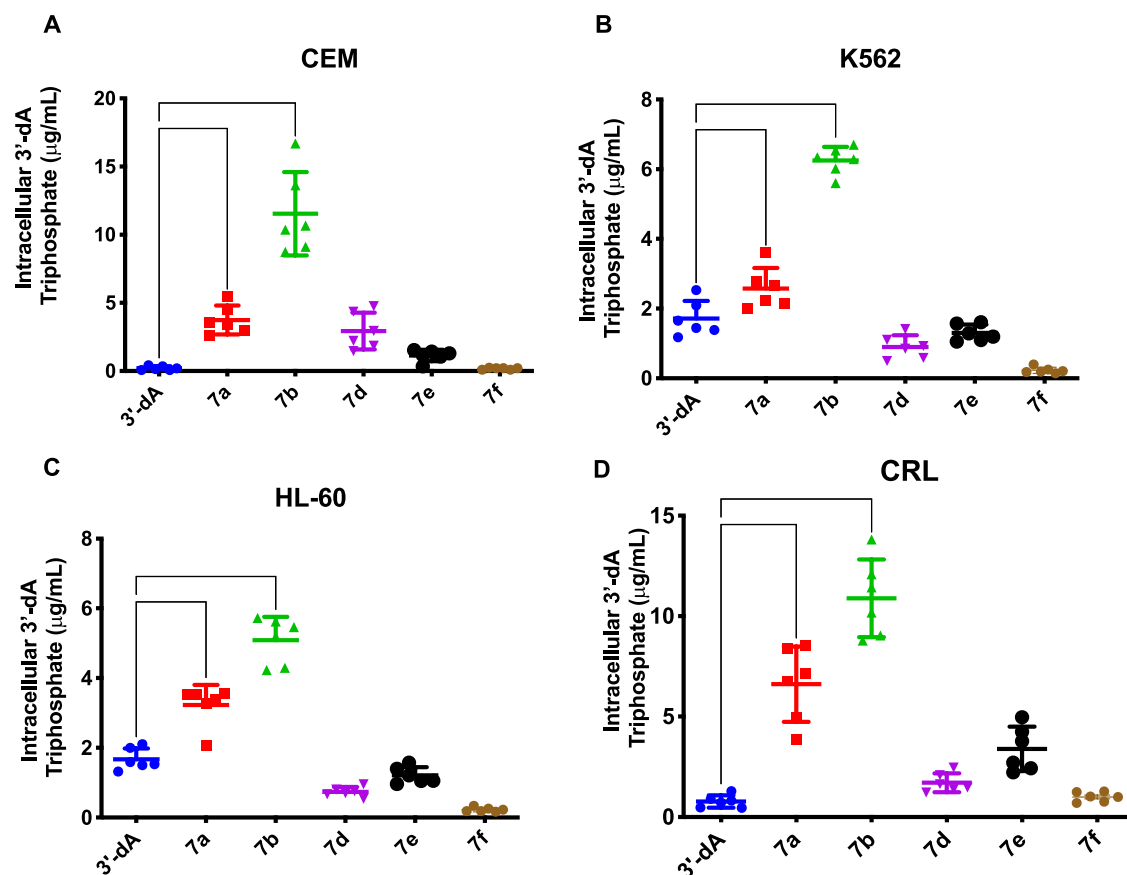


Figure 4. Comparative cytotoxicity of 3'-dA and ProTides 7a,b, d–f in (A) CEM (B), K562 (C), HL-60, and (D) CRL cell lines in the absence of hENT1, AK, and ADA inhibitors.

7b were the most active against this panel of cell lines. The *in vitro* cytotoxic activities of the individual diastereomers 7a-S<sub>p</sub> and 7a-R<sub>p</sub> were similar to their diastereomeric mixture. Phosphorodiamidate 9, although more active than the parental nucleoside, was less potent than the aryloxyphosphoramidates 7a and 7b in all of the cell lines tested.

The *in vitro* cytotoxic activity of the synthesized ProTides and 3'-dA were then evaluated in five hematological cancer cell

lines (CEM, K562, HL60, CRL, and KG1a) (Figure 4) and subsequently, the cytotoxicity observed in 4/5 cell lines (CEM, K562, HL60, CRL) was correlated with the intracellular level of 3'-dATP achieved (measured by liquid chromatography–mass spectrometry). ProTide 7c and phosphorodiamidate 9 were excluded from these studies due to their lack of potency in the cytotoxic screening.



**Figure 5.** Determination of the intracellular accumulation of 3'-dATP after treatment with 3'-dA and prodrugs 7a,b, d–f in the absence of hENT1, AK, and ADA inhibitors. Differences in intracellular triphosphate were assessed in (A) CEM, (B) K562, (C) HL-60, and (D) CRL cell lines, using one-way analysis of variance (ANOVA) with Tukey's correction for multiple comparisons. \*\*\*\*  $P < 0.0001$ , \*\*\*  $P < 0.001$ , \*\*  $P < 0.01$ , \*  $P < 0.05$ .

As depicted in Figure 4A–D, compounds 7a and 7b were the most active ProTides with  $LC_{50}$  values 3- to 150-fold lower than 3'-dA in all four cell lines (Table 2). Compounds 7d and 7e were also more cytotoxic than 3'-dA but were less potent than 7a and 7b. Compound 7f showed only a marginal (1–2-fold) improvement in activity over 3'-dA (Table S2).

The intracellular accumulation of 3'-dATP was associated with the cytotoxicity of each compound. ProTides 7a and 7b generated 3'-dATP intracellular concentrations 3- to 56-fold higher than 3'-dA, whereas 7d and 7e showed only 2- to 15-fold increase in 3'-dATP compared to 3'-dA. Treatment with compound 7f resulted in the lowest 3'-dATP intracellular levels across the four cell lines (Figure 5).

Figure 6 shows the correlation between the cytotoxic activity ( $LC_{50}$  values) of 3'-dA and ProTides 7a,b, d–f, and the intracellular levels of 3'-dATP measured. A strong association between the *in vitro* potency of each agent and the level of intracellular anabolite (3'-dATP) was evident from these studies.

The most active ProTides, 7a and 7b, were next tested for activity and 3'-dATP accumulation in the presence of hENT1, AK, and ADA inhibitors in CEM and CRL, and the results were compared with those obtained for 3'-dA (Figure 7). In the presence of either an hENT1 inhibitor (nitrobenzylthioinosine, NBTI) or an AK inhibitor (A-134974 dihydrochloride hydrate), 3'-dA cytotoxicity was decreased by 2- to 5-fold in both TdT<sup>+</sup> (CEM) and TdT<sup>-</sup> (CRL) cancer cell lines. Conversely, inhibition of ADA with erythro-9-(2-hydroxy-3-nonyl) adenine hydrochloride (EHNA) led to a

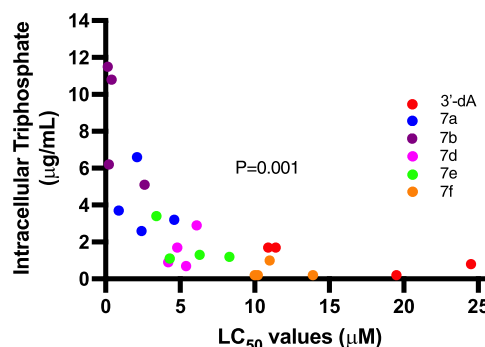


**Figure 6.** Correlation between cytotoxic  $LC_{50}$  values ( $\mu\text{M}$ ) of 3'-dA and compounds 7a,b, d–f and their intracellular 3'-dATP concentrations ( $\mu\text{g/mL}$ ). There was a strong relationship between intracellular triphosphate concentration and  $LC_{50}$  values.

16-fold improvement of 3'-dA  $LC_{50}$  values in CEM and a 2-fold in CRL cell lines. These results indicate the dependency of 3'-dA on hENT1, AK, and ADA activities (Figure S2, Table S2). In contrast, experiments conducted with compounds 7a and 7b were independent of ADA activity as its inhibition by EHNA did not lead to any  $LC_{50}$  changes in CEM cell lines (Figure 7, Table S2). In CRL cell lines, ADA and AK inhibition led to increased 7a cytotoxicity but did not affect 7b. EHNA increased the intracellular 3'-dATP levels generated by 3'-dA by 38- and 19-fold in CEM and CRL cell lines, respectively (Table S2). This indicates that the 3'-dA is rapidly degraded by intracellular ADA. hENT1, AK, and ADA

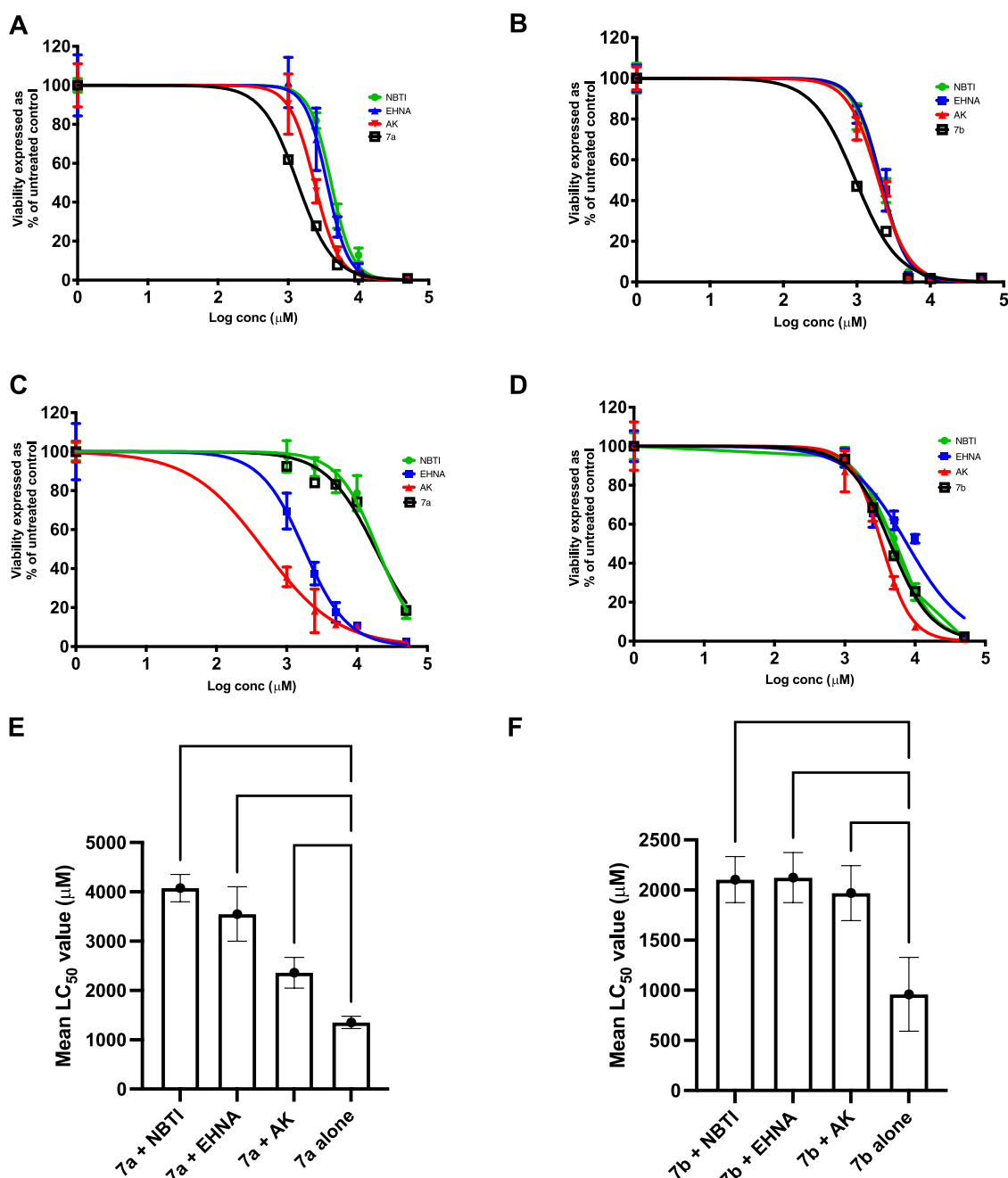


**Figure 7.** Comparative cell viability assay of ProTides 7a and 7b in (A, B) CEM, and (C,D) CRL in the presence of hENT1, AK, and ADA inhibitors. (E, F) Comparative LC<sub>50</sub> values for 7a and 7b, respectively, in the presence and absence of hENT1, AK, and inhibitors in CEM. Statistical analysis was performed using one-way ANOVA with Tukey's correction for multiple comparisons. \*\*\*\**P* < 0.0001, \*\**P* < 0.01, \**P* < 0.05.

inhibitors did not affect the intracellular 3'-dATP levels generated by both ProTides 7a and 7b, which indicates that these new agents can overcome the cancer resistance mechanisms commonly associated with cordycepin (Table S2).

**Leukemic Stem Cell Selectivity.** We have recently reported on the preferential targeting of leukemic stem cells (LSCs) by the gemcitabine ProTide, NUC-1031, in the acute myeloid leukemia cell line KG1a and in primary AML blasts.<sup>62</sup> Therefore, once we evaluated the LC<sub>50</sub> of ProTide 7a and 7b in KG1a cells (Table S2), we went on to assess the relative ability of ProTides 7a and 7b to preferentially kill the LSCs compared to the bulk tumor within the KG1a cell line (LSCs

were defined by the phenotype Lin<sup>-</sup>/CD34<sup>+</sup>/CD38<sup>-</sup>/CD123<sup>+</sup>).<sup>67</sup> While ProTide 7b did not lead to any significant alteration of the proportion of LSCs across the entire range of concentrations, 3'-dA and ProTide 7a showed increased selectivity and potency against the putative leukemic stem cells with 7a significantly reducing the LSC population to a greater extent than the parent nucleoside at concentrations above 1 μM (Figure 8).

**In Vitro Metabolic Stability Study. Stability in Human Hepatocytes.** The metabolic stabilities of 3'-dA ProTides 7a,b,d-f were investigated in human hepatocytes to assess their intrinsic clearances. The results, reported in Table S,

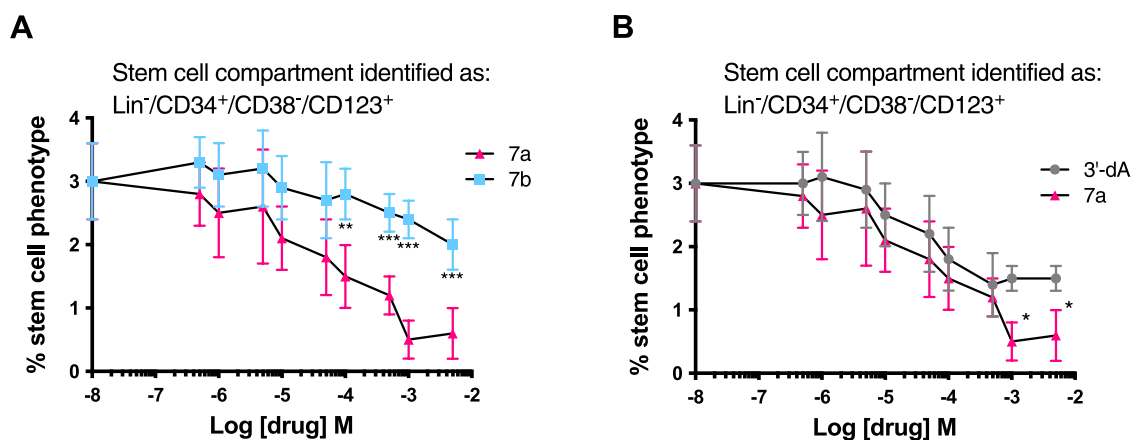


**Figure 8.** Analysis of the LSC-targeting capacity of 3'-dA and ProTides 7a and 7b. The LSC and bulk tumor fractions were identified using a cocktail of antibodies with LSCs: Lin<sup>-</sup>/CD34<sup>+</sup>/CD38<sup>-</sup>/CD123<sup>+</sup> and bulk tumor: Lin<sup>-</sup>/CD34<sup>+</sup>/CD38<sup>+</sup>/CD123<sup>+</sup>. (A) Percentage of viable LSCs remaining in KG1a cell cultures following exposure to increasing concentrations of 7a and 7b. (B) Comparative effects on the LSC pool of 3'-dA and 7a. All data shown are the mean  $\pm$  standard deviation (SD) of three independent experiments. \*\*\*\*  $P < 0.001$ , \*\*  $P < 0.01$ , \*  $P < 0.05$ .

**Table 5. Metabolic Stability of ProTides 7a,b, 7d–f in Human Hepatocytes<sup>a</sup>**

Comp.	Ar	R	R'	R''	$t_{1/2}$	$CL_{int}$
7a	Ph	CH <sub>3</sub>	H	CH <sub>2</sub> Ph	48.1	22.6
7b	1-Napht	CH <sub>3</sub>	H	CH <sub>2</sub> Ph	43.4	20.8
7d	1-Napht	CH <sub>2</sub> CH(CH <sub>3</sub> ) <sub>2</sub>	H	(CH <sub>2</sub> ) <sub>4</sub> CH <sub>3</sub>	71.8	15.8
7e		CH <sub>3</sub>	H	CH <sub>2</sub> Ph	25.6	41.1
7f	1-Napht	CH <sub>3</sub>	CH <sub>3</sub>	CH <sub>3</sub>	96.5	10.0

<sup>a</sup>Half-life ( $t_{1/2}$ ) expressed in minutes; intrinsic clearance ( $CL_{int}$ ) expressed as mL/min/10<sup>6</sup> Cell.

indicate that compounds 7a and 7b have similar half-lives when incubated with human hepatocytes, suggesting that they are processed at the same rate by mammalian carboxylesterases (CES1 and CES2), the crucial enzymes involved in the metabolism of endogenous esters and ester or amide-containing xenobiotics.<sup>68</sup>

In contrast, compound 7e was almost 2-fold less stable (half-life = 26 min) most probably due to the presence of an additional ester moiety at the ortho position of the phenyl ring. Compounds 7d and 7f, bearing an amino acid other than L-alanine, resulted in longer half-lives than the other ProTides, suggesting that the nature of the amino acids plays a role in the carboxylesterase enzyme substrate recognition.

**Deamination by ADA.** Enzymatic evaluation of the stability of compound 7a versus 3'-dA in the presence of ADA was then investigated.<sup>69</sup> As depicted in Figure 9, no shift of the maximum absorption at 265 nm of 7a was observed up to 2 h from the addition of the enzyme solution, confirming the stability of 7a to deamination. In the same condition, 3'-dA showed metabolic deamination completed within 2 minutes from the enzyme addition as evidenced by a shift of the maximum absorption at 259 nm to the maximum absorption at 252 nm, characteristic of the metabolite 3'-dIno (Figure S3).

**Stability in Plasma.** The stability of 3'-dA and compound 7a was assayed in human, dog, mouse, and rat plasma, with or without the presence of EHNA as an ADA inhibitor. When 3'-dA was incubated in human plasma (without the addition of EHNA), the concentration of the compound decreased in a time-dependent manner, until the nucleoside was completely

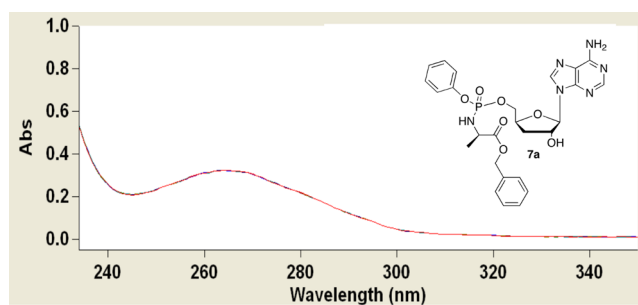


**Figure 9.** UV absorbance spectra of 7a (62.5  $\mu$ M) in the absence (red line) and presence (blue line) of ADA from calf (17 mU/mL<sup>-1</sup>) in phosphate buffer (100 mM, pH 7.4) at 25 °C for 12 h (the two lines are superimposed).

metabolized after 4 h with an estimated half-life of 62 min. When EHNA was added, the stability of 3'-dA was significantly increased, with a 42.1% of 3'-dA remaining after 24 h (Figure S4A). The half-life of 3'-dA was calculated to be 252 min under these circumstances. The metabolism of 3'-dA in mouse plasma, with and without ENHA, followed a similar trend although the nucleoside was metabolized more quickly ( $t_{1/2}$  = 25 min) (Figure S4B). The incubation of ProTide 7a in human plasma showed increased stability compared to the parent nucleoside, with no change in plasma concentration up to 4 h. Moreover, the addition of EHNA did not significantly affect the compound stability (Figure 10A). The stability of 3'-dA and 7a in dog plasma (Figure S5B) was like those found in human plasma (Figure 10A). On the contrary, ProTide 7a

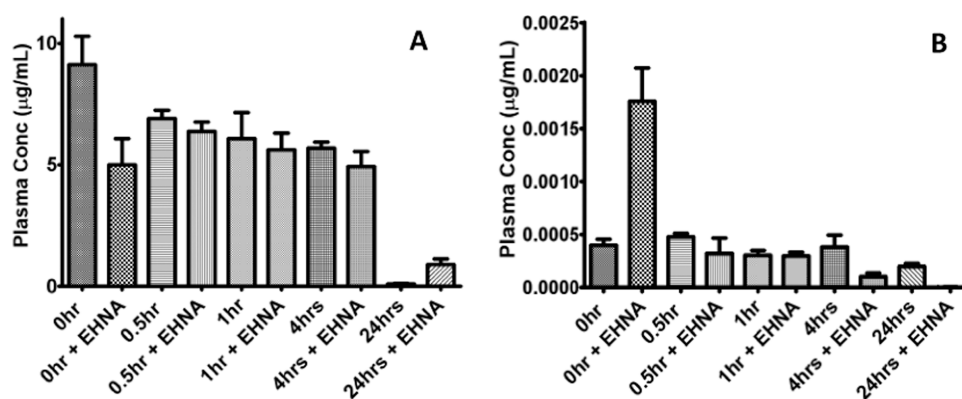


Figure 10. Stability assay of ProTide 7a in human plasma (A) and mouse plasma (B).

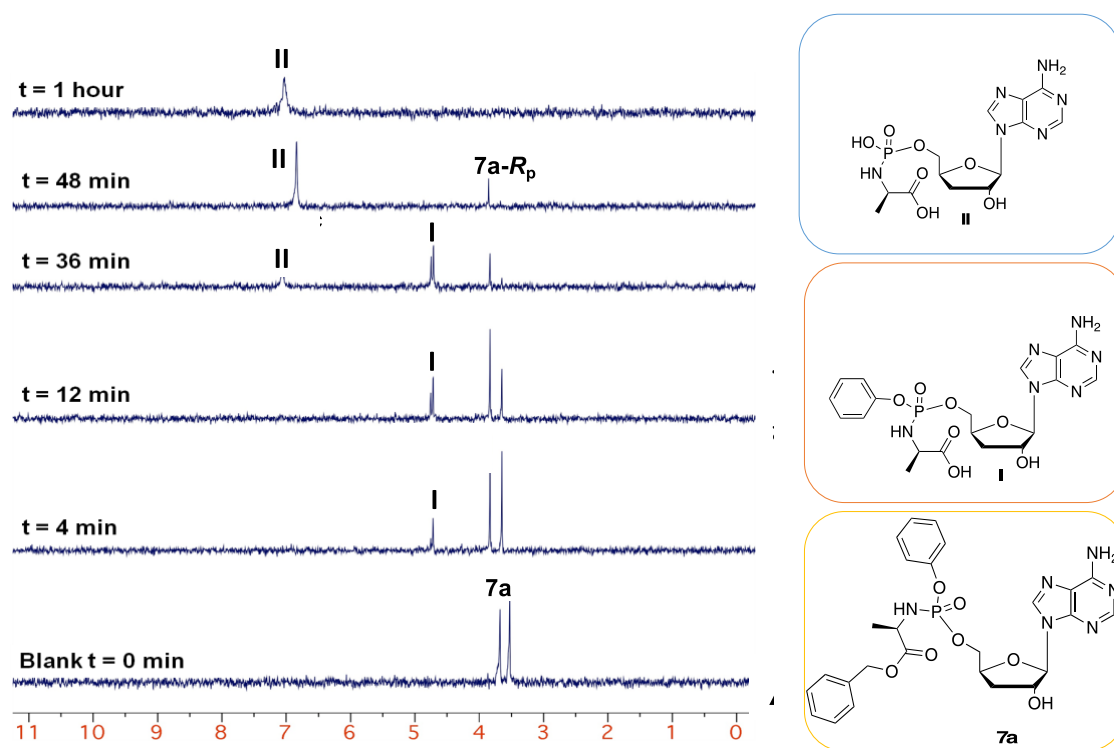


Figure 11. Deconvoluted stacked  $^{31}\text{P}$ -NMR spectra (202 MHz, acetone- $d_6$ /pH 7.6 Trizma buffer) to show the carboxypeptidase-mediated activation of compound 7a to metabolite II over 1 h.

undergoes rapid metabolism in mouse plasma (Figure 10B). In fact, the concentration of this compound was 4 logs lower ( $0.0005 \mu\text{g/mL}$ ) than that detected in human plasma ( $10 \mu\text{g/mL}$ ) after just 30 s of incubation. Moreover, the presence of EHNA did not significantly affect these results, suggesting that the compound is not metabolized by ADA but through other pathways, potentially involving esterase enzymes. It was not possible to estimate the half-life of 7a under these conditions. Similar results to mice plasma (Figure 10B) were obtained in rat plasma (Figure S5A). In fact, higher levels of carboxylesterase enzymes were reported in rodents<sup>70</sup> compared to human, monkey, and dogs, and were suggested to be responsible for the reduced stability of ProTides in *in vivo* mouse xenografts.<sup>33,71</sup>

**Prodrug Activation by Carboxypeptidase.** To exert their cytotoxic activity, ProTides must be metabolized intracellularly to produce the free monophosphate form, which in turn generates the active triphosphate after two

consecutive phosphorylation reactions. In the process of intracellular activation of ProTides, the first step is catalyzed by a carboxylesterase-type enzyme such as Cathepsin A, which was shown to be responsible for the cleavage of the amino acid ester moiety.<sup>72</sup> To prove that the ProTides of 3'-dA are activated in a similar manner, the interaction of compound 7a with a carboxylesterase-type enzyme was investigated. Carboxypeptidase Y was used as a surrogate of Cathepsin A since it belongs to the same family of C-type carboxypeptidases, and it was reported to share similarities in the active site.<sup>73</sup>

Compound 7a was incubated in an NMR tube with carboxypeptidase Y in acetone- $d_6$  in the presence of Trizma buffer (pH 7.6), and the progress of the reaction was monitored by  $^{31}\text{P}$  NMR analyses over 1 h. The stacked spectra, reported in Figure 11, show the formation of two new peaks after 4 min of incubation that correspond to the two diastereoisomers of intermediate I ( $\delta_{\text{P}}$  4.62 and 4.65 ppm,  $t = 4$  min). A complete conversion of the ProTide 7a into the

corresponding aminoacyl phosphoramidate ester **II** ( $\delta_p$  6.89 ppm) was observed after 1 h. The *Sp* diastereoisomer appeared to be converted at a slightly higher rate compared to the *Rp* diastereoisomer. *In vivo*, the aminoacyl phosphoramidate ester metabolite **II** is then believed to undergo P–N bond cleavage, mediated by HINT-1, a phosphoramidase-type enzyme, to eventually release the parental drug in its monophosphate form.<sup>74</sup>

## CONCLUSIONS

A series of phosphoramidate prodrugs of 3'-dA were synthesized and then evaluated for their biological activity against a range of human tumor cell lines. ProTide **7a** and **7b** showed potent cytotoxic activity against a panel of hematological cancer cell lines. Importantly, we demonstrated that both compounds were able to bypass the premature breakdown, the poor uptake, and the kinase dependence for phosphorylation of the parental nucleoside. Compound **7a** (NUC-7738) also showed selective potency against leukemic stem cells, and so it was selected as a clinical candidate drug, which is now the subject of a phase 1/2 clinical trial, NuTide:701, to establish the recommended randomized phase 2 dose and assess safety in patients with advanced solid tumors or lymphoma.<sup>37</sup>

Encouraging PK data from the ongoing phase I/II trial have been already reported, showing that the ProTide NUC-7738 is resistant to ADA degradation and is capable of releasing active 3'-dAMP into cells where it is rapidly converted to the active species 3'-dATP.<sup>34</sup> Preliminary findings from these studies suggest that NUC-7738 is well tolerated and shows encouraging signals of anticancer activity.<sup>34</sup> Taken together, our data show that NUC-7738 overcomes the key cancer resistance mechanisms that limit the efficacy of 3'-dA and support the further clinical evaluation of NUC-7738 as a novel anticancer drug.

## EXPERIMENTAL SECTION

**MTS Cell Viability Assay.** The assay was contracted and carried out by WuXi AppTec (Shanghai) Co., Ltd. The tumor cell lines CCRF-CEM, HL-60, KG-1, MOLT-4, K562, MV4-11, THP-1, HEL92.1.7, NCI-H929, RPMI-8226, Jurkat, Z138, RL, HS445, HepG2, MCF-7, Bx-PC-3, HT29, MIA PaCa-2, and SW620 were seeded at cell densities of 0.5–100 Å and about 103 cells/well in a 96-well plate the day before drug incubation. Then, the plates were incubated for 72 h with the different concentrations of compound to be tested. After the incubation period, 50  $\mu$ L of MTS was added and the tumor cells were incubated for 4 h at 37 °C. The data were read and collected by a Spectra Max 340 absorbance microplate reader. The compounds were tested in duplicate with nine serial concentrations (3.16-fold titrations with 198  $\mu$ M as the highest concentration), and the data were analyzed by XLfit software.

**Adenosine 5'-Triphosphate (ATP) Viability Assay. Cell Culture Conditions.** HL-60 (ATCC CCL-240), K562 (ATCC CCL-243), CCRF-CEM (ATCC CRM-CCL-119), and RL (ATCC CRL-2261) leukemia cell lines were obtained from the American Type Culture Collection (ATCC), Middlesex. HL-60 and K562 cell lines are deoxynucleotidyl transferase-negative (TdT<sup>-ve</sup>), whereas CCRF-CEM cell line is TdT<sup>+ve</sup>. They were cultured in RPMI-1640 medium (Sigma-Aldrich, U.K.), which were supplemented with 10% fetal bovine serum (FBS) (PAA Laboratories), 1% amphotericin B (5.5 mL), and 1% penicillin/streptomycin (5.5 mL) (PAA Laboratories) and grown in flasks at 37 °C in an incubator with 5% CO<sub>2</sub>. For the studies with inhibitors, the cells were treated with 10  $\mu$ M nitrobenzylthioinosine (NBTI, hENT inhibitor) or 1  $\mu$ M EHNA (EHNA hydrochloride) or A-134974 (A-134974 dihydrochloride

hydrate) and left for 5 min before adding the drug. The cells were then incubated for 2 h at 37 °C with 5% CO<sub>2</sub>.

**Measurement of In Vitro Apoptosis.** The amount of ATP was used as a measurement of cell number and cell viability. ATP ViaLight™ plus assay kit (Lonza: Product No. LT07-121) to detect ATP in cells treated in luminescence compatible 96-well plates (initial concentration of cells was 1 × 10<sup>4</sup> cells/well) with Cordycepin and ProTides at concentrations of 0, 0.1, 0.5, 1, 5, and 10  $\mu$ M, followed by incubation for 72 h at 37 °C in an incubator with 5% CO<sub>2</sub>. For inhibitor studies, 10  $\mu$ M NBTI or 1  $\mu$ M EHNA or A-134974 was added and left for 5 min before adding the drugs. After incubation, 50  $\mu$ L of cell lysis reagent was added to the 96-well plates to release the intracellular ATP, followed by 100  $\mu$ L of ATP monitoring reagent (AMR). The luminescent values of each well were determined using FLUOstar OPTIMA microplate reader (BMG Labtech), which converted ATP into light using luciferase enzyme. Therefore, the amount of luminescence produced was directly proportional to the amount of ATP.

**Annexin V/7-AAD Cell Viability Assay. Cell Culture Conditions.** The acute myeloid leukemia (AML) KG1a cell line was maintained in RPMI medium (Invitrogen, Paisley, U.K.) supplemented with 100 units/mL penicillin, 100  $\mu$ g/mL streptomycin, and 20% FBS. Cells were subsequently aliquoted 10<sup>5</sup> cells/100  $\mu$ L into 96-well plates and were incubated at 37 °C in a humidified 5% carbon dioxide atmosphere for 72 h in the presence of 3'-dA and proTides at concentrations that were experimentally determined for each series of compounds. In addition, control cultures were carried out to which no drug was added. The cells were subsequently harvested by centrifugation and were analyzed by flow cytometry using the Annexin V assay. All experiments were performed in triplicate. LC<sub>50</sub> values (the concentration of compound required to kill 50% of the cells in culture) were calculated by nonlinear regression modeling using GraphPad Prism software and are shown as mean ± standard error of the mean (SEM) for each replicate data set.

**3'-dATP Quantification. Cell Treatment and Nucleotide Extraction.** HL-60, K562, CCRF-CEM, and RL leukemic cell lines with 5 × 10<sup>6</sup> cells/mL were used. Cells were treated with 1  $\mu$ L of 50  $\mu$ M of each 3'-dA, **7a,b**, **d–f** and incubated for 2 h at 37 °C with 5% CO<sub>2</sub>. After incubation, the cells were centrifuged (ambient, 300g, 5 min), the culture medium supernatants were removed, and the cell pellets were washed with 1 mL of phosphate-buffered saline (PBS) and centrifuged (ambient, 1200 rpm, 5 min). The supernatants were removed, and the pellets were reconstituted in 100  $\mu$ L of PBS and 100  $\mu$ L of 0.8 M perchloric acid and vortex-mixed and kept on ice for 30 min, then centrifuged (ambient, 300g, 5 min) and 180  $\mu$ L of the supernatant was transferred to new tubes and stored at –80 °C until time of analysis. During analysis, 90  $\mu$ L of the extract was transferred to the fresh tubes. Ammonium acetate (25  $\mu$ L, 1 M) was added to the extract, and then neutralized by the addition of 10  $\mu$ L of 10% ammonia and 5  $\mu$ L of deionized water, then transferred to liquid chromatography–mass spectrometry (LC-MS) vials, and 10  $\mu$ L was injected into the ultrahigh-performance liquid chromatography–tandem mass spectrometry (UPLC-MS/MS) system.

**LC-MS/MS Analysis.** The analytes were resolved using an ultraperformance liquid chromatography system (Accela UPLC, Thermo Scientific, U.K.) equipped with a Biobasic A × 5  $\mu$ m, 50 × 2.1 mm column (Thermo Electron Corporation, Murrieta, CA) and mobile phase consisting of a mixture of 10 mM NH<sub>4</sub>Ac in ACN/H<sub>2</sub>O (30:70 v/v), pH 6.0 (A), and 1 mM NH<sub>4</sub>Ac in ACN/H<sub>2</sub>O (30:70 v/v), pH 10.5 (B). The mobile phase gradient employed comprised buffer A = 95% at 0–0.5 min, from 95 to 0% over 1.25 min, held at 0% for 1.75 min, from 0 to 95% over 0.1 min, ending with 95% for 2.9 min, all at a flow rate of 500  $\mu$ L/min. Eluting compounds of interest were detected using a triple-stage quadrupole Vantage mass spectrometry system (Thermo Scientific, U.K.) equipped with an electrospray ion source. Samples were analyzed in the Multiple Reaction Monitoring, negative-ion modes at a spray voltage of 3000 V. Nitrogen was used as sheath and auxiliary gas at flow rates of 50 and 20 arbitrary units, respectively. Argon was used as collision gas with a pressure of 1.5 mTorr. The optimum transitional daughter ions

mass and collision energy of each analyte were as follows: 3'dATP 490.1 → 392.1 (collision energy 19 V) and the internal standard ChloroATP 539.9 → 442.2 (collision energy 24 V).

**Immunophenotypic Identification of the Leukemic Stem Cells.** KG1a cells were cultured for 72 h in the presence of a wide range of concentrations of 3'-dA and ProTides. Cells were then harvested, and KG1a cells were labeled with anti-CD34 (FITC), anti-CD38 (PE), and anti-CD123 (PERCP cy5). The subpopulation expressing a leukemic stem cell (LSC) phenotype was subsequently identified and was expressed as a percentage of all viable cells left in the culture. The percentages of stem cells remaining were then plotted on a dose–response graph, and the effects of the ProTides were compared with the parental nucleoside to determine if they preferentially target cancer stem cells

**Metabolic Stability. Cryopreserved Human Hepatocytes Assay.** The assay was contracted and performed by Cerep (Seattle, WA Laboratories, 15318 N. E. 95th Street Redmond, WA, 98052) according to the published procedure (Cerep ref 1432). Pooled cryopreserved hepatocytes were thawed, washed, and resuspended in Krebs–Heinslet buffer (pH 7.3). The reaction was initiated by adding the test compound (1 μM final concentration) into cell suspension and incubated in a final volume of 100 μL on a flat-bottom 96-well plate for 0 and 60 min, respectively, at 37 °C/5% CO<sub>2</sub>. The reaction was stopped by adding 100 μL of acetonitrile into the incubation mixture. Samples were then mixed gently and briefly on a plate shaker, transferred completely to a 0.8 mL V-bottom 96-well plate, and centrifuged at 2550g for 15 min at room temperature. Each supernatant (150 μL) was transferred to a clean cluster tube, followed by high-performance liquid chromatography–tandem mass spectrometry (HPLC-MS/MS) analysis on a Thermo Electron triple quadrupole system.

**Plasma Stability.** Plasma samples (10 mL of human, beagle dog, mouse, or rats from Sera laboratories, U.K.) were treated with and without 1 μM of EHNA, after which 20 μM concentration of each drug (3'dA and ProTides) was added and incubated for 2 h at 37 °C with 5% CO<sub>2</sub>. After incubation, 100 μL of each sample was taken and 300 μL of 100% methanol was added and left on ice for 30 min. After 30 min, the mixture was centrifuged (14 000 rpm, 4 °C, 10 min), and the supernatant was transferred to new tubes and evaporated under SpeedVac. Then, the dried extract was reconstituted in 100 μL of 10% acetonitrile, then transferred to LC-MS vials, and 10 μL was injected into the UPLC-MS/MS system.

**Adenosine Deaminase Assay.** Bovine recombinant adenosine deaminase (ADA, EC:3.5.4.4) was purchased from Sigma (Sigma-Aldrich, product number 59722). The ADA suspension (containing >2 U/mL) was aliquoted into 55 μL portions and kept at –20 °C. Before use, a 55 μL sample was thawed and 1 mL of phosphate buffer (0.1 N, pH 7.4) was added. The suspension was filtered through a 0.2 μm filter to remove precipitates that could interfere with the absorbance measurements. The clear supernatant was used for the degradation experiments. The experiments were conducted in UV transparent cuvettes (Sigma-Aldrich, code: Z637092) using an Envision microplate reader (PerkinElmer). Samples contained 62.5 μM of either 3'-dA or ProTide 7a, which were added to 17 μL of the ADA solution. Scans of the absorption spectrum were taken between 220 and 350 nm with 2 nm resolution every 0.1 min over a period of 10 min to 12 h. One sample containing only ADA was also prepared, and this was subtracted to obtain the spectrum over time for substrates.

**Carboxypeptidase Y Assay.** ProTides 7a (5 mg, ±0.008 mmol) was dissolved in 150 μL of acetone-*d*<sub>6</sub>, and 300 μL of trizma buffer (pH 7.6) was added. A <sup>31</sup>P NMR (202 MHz, 64–128 scans) was conducted at this stage as a reference (blank, *t* = 0). To this mixture, 130 μL of a stock solution of carboxypeptidase enzyme (purchased from Sigma-Aldrich, >50 unit/mg, dissolved in trizma buffer pH 7.6 to a concentration of 50 units/mL, EC 3.4.16.1) was added. <sup>31</sup>P NMR (128 scans) were carried out with 1 min of delay between experiments for 14 h at 25 °C.

**Chemistry. General Information.** All solvents used were anhydrous and used as supplied by Sigma-Aldrich. All commercially

available reagents were supplied by either Sigma-Aldrich or Fisher and used without further purification. All solid reagents were dried for several hours under high vacuum prior to use. For analytical thin-layer chromatography (TLC), precoated aluminum-backed plates (60 F-54, 0.2 mm thickness; supplied by E. Merck AG, Darmstadt, Germany) were used and developed by an ascending elution method. For preparative thin-layer chromatography (prep TLC), preparative TLC plates (20 cm × 20 cm, 500–2000 μm) were purchased from Merck. After solvent evaporation, compounds were detected by quenching of the fluorescence at 254 nm upon irradiation with a UV lamp. Column chromatography purifications were carried out by means of automatic Biotage Isolera One. Fractions containing the product were identified by TLC and pooled, and the solvent was removed in vacuo. <sup>1</sup>H, <sup>31</sup>P, and <sup>13</sup>C NMR spectra were recorded in a Bruker Avance 500 spectrometer at 500, 202, and 125 MHz, respectively, and autocalibrated to the deuterated solvent reference peak in case of <sup>1</sup>H and <sup>13</sup>C NMR and 85% H<sub>3</sub>PO<sub>4</sub> for <sup>31</sup>P experiments. All <sup>31</sup>P and <sup>13</sup>C NMR spectra were proton-decoupled. Chemical shifts are given in parts per million (ppm), and coupling constants (*J*) are measured in hertz (Hz). The following abbreviations are used in the assignment of NMR signals: s (singlet), d (doublet), t (triplet), q (quartet), m (multiplet), bs (broad singlet), dd (doublet of doublet), ddd (doublet of doublet of doublet), dt (doublet of triplet). The assignment of the signals in <sup>1</sup>H NMR and <sup>13</sup>C NMR was done based on the analysis of coupling constants and additional two-dimensional experiments (correlation spectroscopy (COSY), heteronuclear single-quantum coherence (HSQC)). Analytical high-performance liquid chromatography (HPLC) analysis was performed using both Spectra System SCM (with X-select-C18, 5 mm, 4.8 × 150 mm column) and Varian Prostar system (LCWorkstation-Varian Prostar 335 LC detector). Preparative HPLC was performed with Varian Prostar (with pursuit XRs C18 150 × 21.2 mm column). Low-resolution mass spectrometry was performed on a Bruker Daltonics MicroToF-LC system (atmospheric pressure ionization, electron spray mass spectroscopy) in positive mode. The ≥95% purity of the final compounds 5a, 6a, 5b, 6b, 7a, 7b, 7c, 7e, and 7f, and the 93% purity for 7d were confirmed using HPLC analysis.

**9-(2',3'-Anhydro-α-D-ribofuranosyl) Adenine (3).** To a stirring suspension of adenosine (2) (10.00 g, 37.42 mmol) in CH<sub>3</sub>CN (250 mL), α-AIBr (22.03 mL, 149.68 mmol, 4 equiv) and H<sub>2</sub>O (0.67 mL, 0.037 mmol, 0.001 equiv) were added, and stirring was continued at room temperature. After 1 h, the mixture was neutralized by the addition of a saturated solution of NaHCO<sub>3</sub> (a change in color from dark orange to clear-white could be noted), and the solution was extracted with EtOAc (2 × 5 mL per mmol of adenosine analogue). The combined organic phase was washed with brine (1 mL × mmol of adenosine analogue). The aqueous phase was extracted with EtOAc (1 × 190 mL), and the combined organic phase was dried over Na<sub>2</sub>SO<sub>4</sub>, filtered, and evaporated to give a white gum. The crude mixture was dissolved in CH<sub>3</sub>OH (260 mL) and stirred for 16 h with Amberlite (2 × OH) resin (150 mL, 1.1 meq/mL by wetted bed volume), previously washed with CH<sub>3</sub>OH. The solution was then filtered, and the resin was carefully washed with CH<sub>3</sub>OH until no spot of the product by TLC could be detected in the filtrate. Evaporation of the combined filtrate and crystallization of the residue from EtOH gave 3 as a white powder (8.86 g, 95%). Melting point 178–180 °C (Lit. mp: 180–181 °C). <sup>1</sup>H NMR (500 MHz, DMSO-*d*<sub>6</sub>) δ<sub>H</sub> 8.33 (s, 1H, H-2), 8.18 (s, 1H, H-8), 7.29 (br s, 2H, NH<sub>2</sub>), 6.21 (s, 1H, H-1'), 5.05 (br s, 1H, OH-5'), 4.46 (d, *J* = 2.6 Hz, 1H, H-2'), 4.22 (d, *J* = 2.6 Hz, 1H, H-3'), 4.18 (t, *J* = 5.2 Hz, 1H, H-4'), 3.60–3.55 (m, 1H, H-5'), 3.53–3.49 (m, 1H, H-5'). <sup>13</sup>C NMR (125 MHz, DMSO-*d*<sub>6</sub>) δ<sub>C</sub> 156.01 (C-6), 152.61 (C-2), 149.11 (C-4), 139.55 (C-8), 119.52 (C-5), 91.25 (C-1'), 81.15 (C-4'), 75.06 (C-2'), 58.75 (C-3'), 57.70 (C-5'). HPLC reversed-phase HPLC eluting with H<sub>2</sub>O/CH<sub>3</sub>CN from 100/0 to 75/25 in 30 min, *F* = 1 mL/min, λ = 254 nm, showed one peak with *t*<sub>R</sub> 13.20 min. C<sub>10</sub>H<sub>13</sub>N<sub>5</sub>O<sub>3</sub> required *m/z* 249.23 [M]; (ES<sup>+</sup>) found *m/z* 272.09 [M + Na]<sup>+</sup>, 250.09 [M + H]<sup>+</sup>.

**3'-Deoxyadenosine (1).** 2',3'-Anhydrous adenosine 3 (9.12 g, 36.59 mmol, 1 equiv) was dissolved in a mixture of DMSO (55 mL) and THF (550 mL), under argon atmosphere. The solution was

cooled down to 0 °C and 1 M LiEt<sub>3</sub>BH in THF (110 mL, 109.77 mmol, 3 equiv) was added dropwise. Stirring was continued at ~4 °C for 1 h and at rt for 16 h. The mixture was cooled down to 0 °C, and an additional portion of 1 M LiEt<sub>3</sub>BH in THF (36.6 mL, 36.6 mmol, 1 equiv) was added dropwise. The mixture was stirred at 0 °C for 1 h and then at rt for 1 h. The reaction mixture was carefully acidified (5% AcOH/H<sub>2</sub>O), purged with N<sub>2</sub> for 1 h (under the fume hood) to remove pyrophoric triethylborane, and evaporated. Purification by silica gel flash column chromatography (eluent system CH<sub>3</sub>OH/CH<sub>2</sub>Cl<sub>2</sub> 5/95 to 20/80) afforded the title compound **1** as a white solid (9.01 g, 98%). Melting point: 188–190 °C (Lit. mp: 191–192 °C). <sup>1</sup>H NMR (500 MHz, DMSO-*d*<sub>6</sub>) δ<sub>H</sub> 8.37 (s, 1H, H-8), 8.17 (s, 1H, H-2), 7.29 (br s, 2H, NH<sub>2</sub>), 5.89 (d, *J* = 2.5 Hz, 1H, H-1'), 5.68 (d, *J* = 4.5 Hz, 1H, OH-2'), 5.19 (t, *J* = 6.0 Hz, 1H, OH-5'), 4.63–4.58 (m, 1H, H-2'), 4.40–4.34 (m, 1H, H-4'), 3.71 (ddd, *J* = 12.0, 6.0, 3.0 Hz, 1H, H-5'), 3.53–3.49 (ddd, *J* = 12.0, 6.0, 4.0 Hz, 1H, H-5'). <sup>13</sup>C NMR (125 MHz, DMSO-*d*<sub>6</sub>) δ<sub>C</sub> 156.00 (C-6), 152.41 (C-2), 148.82 (C-4), 139.09 (C-8), 119.06 (C-5), 90.79 (C-1'), 80.66 (C-4'), 74.56 (C-2'), 62.61 (C-5'), 34.02 (C-3'). C<sub>10</sub>H<sub>13</sub>N<sub>5</sub>O<sub>3</sub> required *m/z* 251.24 [M]. (ES+) found *m/z* 258.12 [M + Li]<sup>+</sup>, 274.09 [M + Na]<sup>+</sup>, 252.11 [M + H]<sup>+</sup>. HPLC reversed-phase eluting with H<sub>2</sub>O/CH<sub>3</sub>CN from 100/0 to 75/25 in 30 min, *F* = 1 mL/min, λ = 254 nm, *t*<sub>R</sub> 11.22 min.

**Standard Procedure A for the Synthesis of Aryl Amino Acid Ester Phosphorochloridates from Amino Acid Hydrochloride or *p*-Toluene Sulfonate Salts.** The appropriate amino acid ester salt (1 equiv) was dissolved in CH<sub>2</sub>Cl<sub>2</sub> (4 mL per mmol of amino acid ester) under argon atmosphere. A solution of the appropriate phosphorodichloridate (1 equiv) in CH<sub>2</sub>Cl<sub>2</sub> (1 mL per mmol of amino acid ester) was added, and the mixture was cooled to –78 °C. Et<sub>3</sub>N (2 equiv) was added dropwise, and the reaction mixture was stirred at –78 °C for 20 min and thereafter at rt for 2.5 h. The solvent was evaporated under reduced pressure, the resulting oil was triturated with anhydrous Et<sub>2</sub>O, and the filtrate was reduced to give the crude product as an oil.

**Phenyl-(benzoxy-*L*-alaninyl)dichlorophosphate (4a).** Prepared according to the general procedure A using *L*-alanine benzyl ester hydrochloride salt (1.12 g, 5.20 mmol), phenyl dichlorophosphate (1.10 g, 5.20 mmol), and Et<sub>3</sub>N (1.45 mL, 10.40 mmol) in CH<sub>2</sub>Cl<sub>2</sub> (20 mL). The product was obtained as a clear oil (1.51 g, 82%). <sup>31</sup>P NMR (202 MHz, CDCl<sub>3</sub>) δ<sub>P</sub> 7.51, 7.85. <sup>1</sup>H NMR (500 MHz, CDCl<sub>3</sub>) δ<sub>H</sub> 7.36–7.25 (m, 10 H, Ar), 5.15 (s, 1H, CH<sub>2</sub>Ph), 5.11 (s, 1H, CH<sub>2</sub>Ph), 4.25–4.14 (m, 2H, NH, CHCH<sub>3</sub>), 1.59–1.57 (m, 3H, CHCH<sub>3</sub>).

**Standard Procedure B for the Synthesis of ProTides 5a,b and 6a,b.** 3'-Deoxyadenosine (**1**) (1 equiv) was dissolved in THF (20 mL per 0.1 mmol of nucleoside) under argon atmosphere. 1 M *t*BuMgCl in THF (1.1 equiv) was added dropwise. The appropriate phosphorochloridate (**4a,b**) (3 equiv) was dissolved in THF (4 mL per 1 mmol of phosphorochloridate), and the resulting solution was added to the initial mixture. The mixture was stirred for 12–16 h, and the solvent was evaporated under vacuum. The obtained crude was purified by silica gel CC or Biotage Isolera One. In some cases, further purification by preparative TLC and/or preparative HPLC was necessary.

**Standard Procedure C for the Synthesis of ProTides 7a–f.** 3'-Deoxyadenosine (**1**) (1 equiv) was dissolved in THF (7 mL per 0.1 mmol of nucleoside) under argon atmosphere. The appropriate phosphorochloridate (**4a–f**) (3 equiv) was dissolved in THF (4 mL per 1 mmol of phosphorochloridate), and the resulting solution was added to the initial mixture, followed by NMI (5 equiv). The mixture was stirred for 12–16 h, and the solvent was evaporated under vacuum. The obtained crude was purified by silica gel CC or Biotage Isolera One. In some cases, further purification by preparative TLC and/or preparative HPLC was necessary.

**(*R*<sub>p</sub>)- and (*S*<sub>p</sub>)-3'-Deoxyadenosine 5'-*O*-phenyl-(benzoxy-*L*-alaninyl)-phosphate (7a).** Prepared according to general procedure C using 3'-deoxyadenosine (**1**) (0.05 g, 0.20 mmol) in anhydrous THF (4 mL), *N*-methyl imidazole (0.080 μL, 1.0 mmol), and phenyl-(benzyloxy-*L*-alaninyl) phosphorochloridate (**4a**) (0.021 g, 0.6 mmol) in THF (2.4 mL). Purification by Biotage Isolera One (cartridge

SNAP 25 g, 25 mL/min, CH<sub>3</sub>OH/CH<sub>2</sub>Cl<sub>2</sub> 1–8% 10 CV, 8% 5 CV) and preparative TLC (1000 μM, eluent system CH<sub>3</sub>OH/CH<sub>2</sub>Cl<sub>2</sub> 5/95) afforded the title compound **7a** as a white solid (0.032 g, 28%). <sup>31</sup>P NMR (202 MHz, CD<sub>3</sub>OD) δ<sub>P</sub> 3.91, 3.73. <sup>1</sup>H NMR (500 MHz, CDCl<sub>3</sub>) δ<sub>H</sub> 8.26 (s, 0.5H, H-8), 8.24 (s, 0.5H, H-8), 8.22 (s, 0.5H, H-2), 8.21 (s, 0.5H, H-2), 7.34–7.25 (m, 7H, Ar), 7.21–7.13 (m, 3H, Ar), 6.01 (d, *J* = 1.5 Hz, 0.5H, H-1'), 6.00 (d, *J* = 1.5 Hz, 0.5H, H-1'), 5.15–5.04 (m, 2H, CH<sub>2</sub>Ph), 4.73–4.63 (m, 2H, H-2', H-4'), 4.43–4.35 (m, 1H, H-5'), 4.27–4.20 (m, 1H, H-5'), 4.03–3.91 (m, 1H, CHCH<sub>3</sub>), 2.35–2.28 (m, 1H, H-3'), 2.09–2.02 (m, 1H, H-3'), 1.32 (d, *J* = 7.4 Hz, 1.5 H, CHCH<sub>3</sub>), 1.28 (d, *J* = 7.4 Hz, 1.5 H, CHCH<sub>3</sub>). <sup>13</sup>C NMR (125 MHz, CD<sub>3</sub>OD) δ<sub>C</sub> 174.84 (d, <sup>3</sup>*J*<sub>C-P</sub> = 4.5 Hz, C=O), 174.63 (d, <sup>3</sup>*J*<sub>C-P</sub> = 4.5 Hz, C=O), 157.32 (C-6), 157.31 (C-6), 153.86 (C-2), 153.84 (C-2), 152.13 (C-4), 152.07 (C-4), 150.20 (C-Ar), 150.18 (C-Ar), 140.47 (C-8), 137.26 (C-Ar), 137.19 (C-Ar), 130.76 (CH-Ar), 130.74 (CH-Ar), 129.57 (CH-Ar), 129.32 (CH-Ar), 129.31 (CH-Ar), 129.29 (CH-Ar), 129.26 (CH-Ar), 126.16 (CH-Ar), 126.14 (CH-Ar), 121.46 (d, <sup>3</sup>*J*<sub>C-P</sub> = 4.7 Hz, CH-Ar), 121.38 (d, <sup>3</sup>*J*<sub>C-P</sub> = 4.7 Hz, CH-Ar), 120.54 (C-5), 120.53 (C-5), 93.24 (C-1'), 93.18 (C-1'), 80.43 (d, <sup>3</sup>*J*<sub>C-P</sub> = 3.6 Hz, C-4'), 80.36 (d, <sup>3</sup>*J*<sub>C-P</sub> = 3.6 Hz, C-4'), 76.62 (C-2'), 68.62 (d, <sup>2</sup>*J*<sub>C-P</sub> = 5.3 Hz, C-5'), 68.30 (d, <sup>2</sup>*J*<sub>C-P</sub> = 5.3 Hz, C-5'), 67.95 (CH<sub>2</sub>Ph), 67.92 (CH<sub>2</sub>Ph), 51.74 (CHCH<sub>3</sub>), 51.60 (CHCH<sub>3</sub>), 34.91 (C-3'), 34.70 (C-3'), 20.45 (d, <sup>3</sup>*J*<sub>C-P</sub> = 7.0 Hz, CHCH<sub>3</sub>), 20.28 (d, <sup>3</sup>*J*<sub>C-P</sub> = 7.0 Hz, CHCH<sub>3</sub>). Reversed-phase HPLC eluting with H<sub>2</sub>O/CH<sub>3</sub>CN from 100/10 to 0/100 in 30 min, *F* = 1 mL/min, λ = 254 nm, *t*<sub>R</sub> 13.56 and 13.75 min. C<sub>26</sub>H<sub>29</sub>N<sub>6</sub>O<sub>5</sub>P required *m/z* 568.2 [M]. MS (ES+) found *m/z* 569.2 [M + H]<sup>+</sup>, 591.2 [M + Na]<sup>+</sup>, 1159.4 [2M+Na]<sup>+</sup>.

The two diastereoisomers **7a-R<sub>p</sub>** and **7a-S<sub>p</sub>** were separated via Biotage Isolera One (cartridge SNAP-Ultra C18 12 g, *F*: 12 mL/min, isotactic eluent system: H<sub>2</sub>O/CH<sub>3</sub>OH 45/55 in 30 min, 150 mg sample) to obtain:

**7a-R<sub>p</sub> as Fast Eluting Isomer (76 mg).** <sup>31</sup>P NMR (202 MHz, CD<sub>3</sub>OD) δ<sub>P</sub> 3.91. <sup>1</sup>H NMR (500 MHz, CDCl<sub>3</sub>) δ<sub>H</sub> 8.26 (s, 1H, H-8), 8.22 (s, 1H, H-2), 7.37–7.25 (m, 7H, Ar), 7.22–7.12 (m, 3H, Ar), 6.01 (d, *J* = 1.5 Hz, 1H, H-1'), 5.12 (AB q, *J*<sub>AB</sub> = 12.0 Hz, 2H, CH<sub>2</sub>Ph), 4.74–4.70 (m, 1H, H-2'), 4.69–4.62 (m, 1H, H-4'), 4.44–4.38 (m, 1H, H-5'), 4.28–4.21 (m, 1H, H-5'), 3.99–3.90 (m, 1H, CHCH<sub>3</sub>), 2.35–2.27 (m, 1H, H-3'), 2.09–2.02 (m, 1H, H-3'), 1.29 (d, *J* = 7.0 Hz, 3H, CHCH<sub>3</sub>). HPLC reversed-phase HPLC eluting with H<sub>2</sub>O/CH<sub>3</sub>CN from 90/10 to 0/100 in 30 min, *F* = 1 mL/min, λ = 254 nm, showed one peak with *t*<sub>R</sub> 13.56 min.

**7a-S<sub>p</sub> as Slow-Eluting Isomer (61 mg).** <sup>31</sup>P NMR (202 MHz, CD<sub>3</sub>OD) δ<sub>P</sub> 3.73. <sup>1</sup>H NMR (500 MHz, CDCl<sub>3</sub>) δ<sub>H</sub> 8.24 (s, 1H, H-8), 8.22 (s, 1H, H-2), 7.36–7.26 (m, 7H, Ar), 7.22–7.13 (m, 3H, Ar), 6.01 (d, *J* = 1.5 Hz, 1H, H-1'), 5.08 (AB q, *J*<sub>AB</sub> = 12.0 Hz, 2H, CH<sub>2</sub>Ph), 4.70–4.67 (m, 1H, H-2'), 4.66–4.60 (m, 1H, H-4'), 4.41–4.35 (m, 1H, H-5'), 4.26–4.19 (m, 1H, H-5'), 4.02–3.94 (m, 1H, CHCH<sub>3</sub>), 2.36–2.27 (m, 1H, H-3'), 2.08–2.01 (m, 1H, H-3'), 1.34–1.30 (m, 3H, CHCH<sub>3</sub>). HPLC reversed-phase HPLC eluting with H<sub>2</sub>O/CH<sub>3</sub>CN from 90/10 to 0/100 in 30 min, *F* = 1 mL/min, λ = 254 nm, *t*<sub>R</sub> 13.75 min.

## ■ ASSOCIATED CONTENT

### Supporting Information

The Supporting Information is available free of charge at <https://pubs.acs.org/doi/10.1021/acs.jmedchem.2c01348>.

Antiproliferative activity of 3'-dA and compounds **5a,b** and **6b** (Table S1); antiproliferative activity of compounds **7a,b, d–f** in CEM, K562, HL60, CRL cell lines (Table S2); antiproliferative activity and 3'-dATP level of 3'-dA and compounds **7a,b** in the presence of NBTI, EHNA, and A-134974 dihydrochloride hydrate in CEM and CRL cell lines (Table S3); analytical HPLC traces of **7a** diastereomeric mixture (Figure S1); in vitro cytotoxicity of 3'-dA in the presence/absence of hENT3, AK, and ADA blockers in CEM and CRL cell lines

(Figure S2); change in UV absorbance spectra of 3'-dA after addition of a solution of ADA (in phosphate buffer pH 7.4) (Figure S3); stability of 3'-dA in human and mouse plasma (Figure S4); stability of 3'-dA and 7a in rat and dog plasma (Figure S5); intermediate and final compounds characterization description; copies of <sup>31</sup>P, <sup>1</sup>H, and <sup>13</sup>C NMR spectra, and HPLC traces of compounds 1, 3, 5a–b, 7a–f, 7a-Rp and 7a-Sp, and 9; atomic coordinates and equivalent isotropic displacement parameters for Sp-7a (PDF)

Molecular formula strings (CSV)

## AUTHOR INFORMATION

### Corresponding Author

Michaela Serpi – School of Chemistry, Cardiff University  
Main Building, Cardiff CF10 3AT Wales, U.K.;  
orcid.org/0000-0002-6162-7910; Email: serpim5@cardiff.ac.uk

### Authors

Valentina Ferrari – School of Pharmacy and Pharmaceutical Sciences, Cardiff University, Cardiff CF10 3NB, U.K.

Christopher McGuigan – School of Pharmacy and Pharmaceutical Sciences, Cardiff University, Cardiff CF10 3NB, U.K.

Essam Ghazaly – Centre for Haemato-Oncology, Barts Cancer Institute, Queen Mary University of London, London EC1M 6BQ, U.K.

Chris Pepper – Brighton and Sussex Medical School, University of Sussex, Brighton BN1 9PX, U.K.

Complete contact information is available at:  
<https://pubs.acs.org/10.1021/acs.jmedchem.2c01348>

### Author Contributions

Experimental design, execution, data interpretation, and presentation were conducted by M.S., V.F., E.G., and C.P. The manuscript was written by M.S. with input from V.F., E.G., and C.P. C.M. supervised the project. E.G. and C.P. contributed equally as last authors. All authors have given approval to the final version of the manuscript.

### Notes

The authors declare no competing financial interest.

## ACKNOWLEDGMENTS

The authors thank NuCana plc for funding part of the research work described in this manuscript. They acknowledge Wuxi AppTec and CEREP for some of the biological evaluations contained within this manuscript.

## ABBREVIATIONS USED

ADA, adenosine deaminase; ADORAs, adenosine receptors; AK, adenosine kinase; AMPK, adenosine monophosphate kinase; 3'-dA, 3'-deoxyadenosine; 3'-dAMP, 3'-deoxyadenosine monophosphate; 3'-dATP, 3'-deoxyadenosine triphosphate; DRs, death receptors; EGFR, epidermal growth factor receptor; hENT, human equilibrative nucleoside transporters; NDPK, nucleoside diphosphate kinases; 3'-dIno, 3'-deoxyinosine; PAP, polyadenylate polymerase; PRPPT, phosphoribosyl-pyrophosphate aminotransferase

## REFERENCES

- (1) Paterson, R. R. M. Cordyceps: a traditional Chinese medicine and another fungal therapeutic biofactory. *Phytochemistry* **2008**, *69*, 1469–1495.
- (2) Tah, J. Cordyceps, an endangered medicinal Plant. *World J. Pharm. Pharm. Sci.* **2017**, *6*, 572–593.
- (3) Tuli, H. S.; Sharma, A. K.; Sandhu, S. S.; Kashyap, D. Cordycepin: a bioactive metabolite with therapeutic potential. *Life Sci.* **2013**, *93*, 863.
- (4) Tuli, H. S.; Sandhu, S. S.; Sharma, A. K. Pharmacological and therapeutic potential of Cordyceps with special reference to Cordycepin. *3 Biotech* **2014**, *4*, 1–12.
- (5) Khan, M. A.; Tania, M.; Zhang, D.-Z.; Chen, H.-C. Cordyceps Mushroom: A Potent Anticancer Nutraceutical. *Open Nutraceuticals J.* **2010**, *3*, 179–183.
- (6) Nakamura, K.; Shinozuka, K.; Yoshikawa, N. Anticancer and antimetastatic effects of cordycepin, an active component of Cordyceps sinensis. *J. Pharmacol. Sci.* **2015**, *127*, 53.
- (7) Yoon, S. Y.; Park, S. J.; Park, Y. J. The Anticancer Properties of Cordycepin and Their Underlying Mechanisms. *Int. J. Mol. Sci.* **2018**, *19*, 3027.
- (8) Qin, P.; Li, X.; Yang, H.; Wang, Z.-Y.; Lu, D. Therapeutic Potential and Biological Applications of Cordycepin and Metabolic Mechanisms in Cordycepin-Producing Fungi. *Molecules* **2019**, *24*, 2231.
- (9) Shelton, J.; Lu, X.; Hollenbaugh, J. A.; Cho, J. H.; Amblard, F.; Schinazi, R. F. Metabolism, Biochemical Actions, and Chemical Synthesis of Anticancer Nucleosides, Nucleotides, and Base Analogs. *Chem. Rev.* **2016**, *116*, 14379–14455.
- (10) Holbein, S.; Wengi, A.; Decourty, L.; Freimoser, F. M.; Jacquier, A.; Dichtl, B. Cordycepin interferes with 3' end formation in yeast independently of its potential to terminate RNA chain elongation. *RNA* **2009**, *15*, 837–849.
- (11) Tsai, Y.-J.; Lin, L.-C.; Tsai, T.-H. Pharmacokinetics of Adenosine and Cordycepin, a Bioactive Constituent of Cordyceps sinensis in Rat. *J. Agric. Food Chem.* **2010**, *58*, 4638–4643.
- (12) Mikhailopulo, I. A.; Wiedner, H.; Cramer, F. Substrate specificity of adenosine deaminase: the role of the substituents at the 2'- and 3'-carbons of adenine nucleosides, of their configuration and of the conformation of the furanose ring. *Biochem. Pharmacol.* **1981**, *30*, 1001–1004.
- (13) Li, G.; Nakagome, I.; Hirono, S.; Itoh, T.; Fujiwara, R. Inhibition of adenosine deaminase (ADA)-mediated metabolism of cordycepin by natural substances. *Pharmacol. Res. Perspect.* **2015**, *3*, No. e00121.
- (14) Wang, Z.; Wu, X.; Liang, Y. N.; Wang, L.; Song, Z. X.; Liu, J. L.; Tang, Z. S. Cordycepin Induces Apoptosis and Inhibits Proliferation of Human Lung Cancer Cell Line H1975 via Inhibiting the Phosphorylation of EGFR. *Molecules* **2016**, *21*, 1267.
- (15) Rottman, F.; Guarino, A. J. The inhibition of phosphoribosylpyrophosphate amidotransferase activity by cordycepin monophosphate. *Biochim. Biophys. Acta* **1964**, *89*, 465–472.
- (16) Wu, W.-D.; Hu, Z.-M.; Shang, M.-J.; Zhao, D.-J.; Zhang, C.-W.; Hong, D.-F.; Huang, D.-S. Cordycepin Down-Regulates Multiple Drug Resistant (MDR)/HIF-1 $\alpha$  through Regulating AMPK/mTORC1 Signaling in GBC-SD Gallbladder Cancer Cells. *Int. J. Mol. Sci.* **2014**, *15*, 12778–12790.
- (17) Chen, Y.; Yang, S. H.; Hueng, D. Y.; Syu, J. P.; Liao, C. C.; Wu, Y. C. Cordycepin induces apoptosis of C6 glioma cells through the adenosine 2A receptor-p53-caspase-7-PARP pathway. *Chem. Biol. Interact.* **2014**, *216*, 17–25.
- (18) Cao, H.-L.; Liu, Z.-J.; Chang, Z. Cordycepin induces apoptosis in human bladder cancer cells via activation of A3 adenosine receptors. *Tumour Biol.* **2017**, *39*, No. 101042831770691.
- (19) Nakamura, K.; Yoshikawa, N.; Yamaguchi, Y.; Kagota, S.; Shinozuka, K.; Kunitomo, M. Antitumor effect of cordycepin (3'-deoxyadenosine) on mouse melanoma and lung carcinoma cells involves adenosine A3 receptor stimulation. *Anticancer Res.* **2006**, *26*, 43–47.

- (20) Lee, S. Y.; Debnath, T.; Kim, S. K.; Lim, B. O. Anti-cancer effect and apoptosis induction of cordycepin through DR3 pathway in the human colonic cancer cell HT-29. *Food Chem. Toxicol.* **2013**, *60*, 439–447.
- (21) Lee, H. H.; Kim, S. O.; Kim, G. Y.; Moon, S. K.; Kim, W. J.; Jeong, Y. K.; Yoo, Y. H.; Choi, Y. H. Involvement of autophagy in cordycepin-induced apoptosis in human prostate carcinoma LNCaP cells. *Environ. Toxicol. Pharmacol.* **2014**, *38*, 239–250.
- (22) Tsesmetzis, N.; Paulin, C. B. J.; Rudd, S. G.; Herold, N. Nucleobase and Nucleoside Analogues: Resistance and Re-Sensitisation at the Level of Pharmacokinetics, Pharmacodynamics and Metabolism. *Cancers* **2018**, *10*, 240.
- (23) Hawley, S. A.; Ross, F. A.; Russell, F. M.; Atrih, A.; Lamont, D. J.; Hardie, D. G. Mechanism of Activation of AMPK by Cordycepin. *Cell Chem. Biol.* **2020**, *27*, 214–222.
- (24) Boston Medical Center. A Phase I Study of Cordycepin (NSC 63984) Plus 2'-Deoxycoformycin (NSC 218321) in Patients With Refractory TdT-Positive Leukemia In: ClinicalTrials.gov [internet] National Library of Medicine [cited 2022 March 31] available from: <https://clinicaltrials.gov/ct2/show/NCT00709215>. NLM identifier: NCT00709215.
- (25) Boston Medical Center. Chemotherapy With Cordycepin Plus Pentostatin in Treating Patients With Refractory Acute Lymphocytic or Chronic Myelogenous Leukemia In: ClinicalTrials.gov [internet] National Library of Medicine [cited 2022 March 31] available from: <https://clinicaltrials.gov/ct2/show/NCT00003005>. NLM identifier: NCT00003005.
- (26) Serpi, M.; Pertusati, F. An overview of ProTide technology and its implications to drug discovery. *Expert Opin. Drug Discovery* **2021**, *16*, 1149–1161.
- (27) Slusarczyk, M.; Serpi, M.; Pertusati, F. Phosphoramidates and phosphonamides (ProTides) with antiviral activity. *Antiviral Chem. Chemother.* **2018**, *26*, No. 2040206618775243.
- (28) Bhatia, H. K.; Singh, H.; Grewal, N.; Natt, N. K. Sofosbuvir: A novel treatment option for chronic hepatitis C infection. *J. Pharmacol. Pharmacother.* **2014**, *5*, 278–284.
- (29) Ray, A. S.; Fordyce, M. W.; Hitchcock, M. J. Tenofovir alafenamide: A novel prodrug of tenofovir for the treatment of Human Immunodeficiency Virus. *Antiviral Res.* **2016**, *125*, 63–70.
- (30) Beigel, J. H.; Tomashek, K. M.; Dodd, L. E.; Mehta, A. K.; Zingman, B. S.; Kalil, A. C.; Hohmann, E.; Chu, H. Y.; Luetkemeyer, A.; Kline, S.; Lopez de Castilla, D.; Finberg, R. W.; Dierberg, K.; Tapon, V.; Hsieh, L.; Patterson, T. F.; Paredes, R.; Sweeney, D. A.; Short, W. R.; Touloumi, G.; Lye, D. C.; Ohmagari, N.; Oh, M.-d.; Ruiz-Palacios, G. M.; Benfield, T.; Fätkenheuer, G.; Kortepeter, M. G.; Atmar, R. L.; Creech, C. B.; Lundgren, J.; Babiker, A. G.; Pett, S.; Neaton, J. D.; Burgess, T. H.; Bonnett, T.; Green, M.; Makowski, M.; Osinusi, A.; Nayak, S.; Lane, H. C. N. Remdesivir for the Treatment of Covid-19 — Final Report. *N. Engl. J. Med.* **2020**, *383*, 1813–1826.
- (31) Slusarczyk, M.; Lopez, M. H.; Balzarini, J.; Mason, M.; Jiang, W. G.; Blagden, S.; Thompson, E.; Ghazaly, E.; McGuigan, C. Application of ProTide Technology to Gemcitabine: A Successful Approach to Overcome the Key Cancer Resistance Mechanisms Leads to a New Agent (NUC-1031) in Clinical Development. *J. Med. Chem.* **2014**, *57*, 1531–1542.
- (32) Blagden, S. P.; Rizzuto, I.; Suppiah, P.; O'Shea, D.; Patel, M.; Spiers, L.; Sukumaran, A.; Bharwani, N.; Rockall, A.; Gabra, H.; El-Bahrawy, M.; Wasan, H.; Leonard, R.; Habib, N.; Ghazaly, E. Antitumour activity of a first-in-class agent NUC-1031 in patients with advanced cancer: results of a phase I study. *Br. J. Cancer* **2018**, *119*, 815–822.
- (33) McGuigan, C.; Murziani, P.; Slusarczyk, M.; Gonczy, B.; Vande Voorde, J.; Liekens, S.; Balzarini, J. Phosphoramidate ProTides of the Anticancer Agent FUDR Successfully Deliver the Preformed Bioactive Monophosphate in Cells and Confer Advantage over the Parent Nucleoside. *J. Med. Chem.* **2011**, *54*, 7247–7258.
- (34) Schwenzer, H.; De Zan, E.; Elshani, M.; van Stiphout, R.; Kudsy, M.; Morris, J.; Ferrari, V.; Um, I. H.; Chettle, J.; Kazmi, F.; Campo, L.; Easton, A.; Nijman, S.; Serpi, M.; Symeonides, S.; Plummer, R.; Harrison, D. J.; Bond, G.; Blagden, S. P. The novel nucleoside analogue ProTide NUC-7738 overcomes cancer resistance mechanisms in vitro and in a first-in-human Phase I clinical trial. *Clin. Cancer Res.* **2021**, *27*, 6500–6513.
- (35) University of Oxford. NUC-3373 in Advanced Solid Tumours (NuTide:301). In: ClinicalTrials.gov [internet] National Library of Medicine [cited 2022 March 31] available from: <https://clinicaltrials.gov/ct2/show/NCT02723240>. NLM identifier: NCT02723240.
- (36) NuCana plc. A Safety Study of NUC-3373 in Combination With Standard Agents Used in Colorectal Cancer Treatment In: ClinicalTrials.gov [internet] National Library of Medicine [cited 2022 March 31] available from: <https://clinicaltrials.gov/ct2/show/NCT03428958>. NLM identifier: NCT03428958.
- (37) Imperial College London. NUC-1031 in Patients With Advanced Solid Tumours (ProGem1) In: ClinicalTrials.gov [internet] National Library of Medicine [cited 2022 March 31] available from: <https://www.clinicaltrials.gov/ct2/show/NCT01621854>. NLM identifier: NCT01621854.
- (38) NuCana plc. NUC-1031 of Nuc-1031 and Carboplatin Combination to Treat Recurrent Ovarian Cancer (ProGem2) In: ClinicalTrials.gov [internet] National Library of Medicine [cited 2022 March 31] available from: <https://clinicaltrials.gov/ct2/show/NCT02303912>. NLM identifier: NCT02303912.
- (39) NuCana plc. NUC-1031 in Patients With Platinum-Resistant Ovarian Cancer. In: ClinicalTrials.gov [internet] National Library of Medicine [cited 2022 March 31] available from: <https://www.clinicaltrials.gov/ct2/show/NCT03146663>. NLM identifier: NCT03146663.
- (40) The Christie NHS Foundation Trust. ABC-08: Phase Ib Trial of Acelarin in Combination with Cisplatin in Locally Advanced/Metastatic Biliary Tract Cancers (ABC-08). In: ClinicalTrials.gov [internet] National Library of Medicine [cited 2022 March 31] available from: <https://www.clinicaltrials.gov/ct2/show/NCT02351765>. NLM identifier: NCT 02351765.
- (41) NuCana plc. A Safety Study of NUC-7738 in Patients With Advanced Solid Tumours or Lymphoma. In: ClinicalTrials.gov [internet] National Library of Medicine [cited 2022 March 31] available from: <https://www.clinicaltrials.gov/ct2/show/NCT03829254>. NLM identifier: NCT03829254.
- (42) Walton, E.; Nutt, R. F.; Jenkins, S. R.; Holly, F. W. 3'-Deoxynucleosides. I. A Synthesis of 3'-Deoxyadenosine. *J. Am. Chem. Soc.* **1964**, *86*, 2952.
- (43) McDonald, F. E.; Gleason, M. M. Asymmetric Synthesis of Nucleosides via Molybdenum-Catalyzed Alkynol Cycloisomerization Coupled with Stereoselective Glycosylations of Deoxyfuranose Glycals and 3-Amidofuranose Glycals. *J. Am. Chem. Soc.* **1996**, *118*, 6648–6659.
- (44) Ito, Y.; Shibata, T.; Arita, M.; Sawai, H.; Ohno, M. Chirally selective synthesis of sugar moiety of nucleosides by chemicoenzymatic approach: L- and D-riboses, showdomycin, and cordycepin. *J. Am. Chem. Soc.* **1981**, *103*, 6739–6741.
- (45) Wang, Z.; Prudhomme, D. R.; Buck, J. R.; Park, M.; Rizzo, C. J. Stereocontrolled Syntheses of Deoxyribonucleosides via Photo-induced Electron-Transfer Deoxygenation of Benzoyl-Protected Ribo- and Arabinonucleosides. *J. Org. Chem.* **2000**, *65*, 5969–5985.
- (46) Todd, A.; Ulbricht, T. L. V. 656. Deoxynucleosides and related compounds. Part IX. A synthesis of 3'-deoxyadenosine. *J. Chem. Soc.* **1960**, 3275–3277.
- (47) Hansske, F.; J Robins, M. Regiospecific and stereoselective conversion of ribonucleosides to 3'-deoxynucleosides. A high yield three-stage synthesis of cordycepin from adenosine. *Tetrahedron Lett.* **1985**, *26*, 4295–4298.
- (48) Meier, C.; Huynh-Dinh, T. Improved Conversion of Adenosine to 3'-Deoxyadenosine. *Synlett* **1991**, 1991, 227–228.
- (49) Aman, S.; Anderson, D. J.; Connolly, T. J.; Crittall, A. J.; Ji, G. From Adenosine to 3'-Deoxyadenosine: Development and Scale Up. *Org. Process Res. Dev.* **2000**, *4*, 601–605.
- (50) Moreau, C.; Kirchberger, T.; Swarbrick, J. M.; Bartlett, S. J.; Fliegert, R.; Yorgan, T.; Bauche, A.; Harnett, A.; Guse, A. H.; Potter,

- B. V. L. Structure–Activity Relationship of Adenosine 5′-diphosphoribose at the Transient Receptor Potential Melastatin 2 (TRPM2) Channel: Rational Design of Antagonists. *J. Med. Chem.* **2013**, *56*, 10079–10102.
- (51) Serpi, M.; Madela, K.; Pertusati, F.; Slusarczyk, M. Synthesis of Phosphoramidate Prodrugs: ProTide Approach. *Curr. Protoc. Nucleic Acid Chem.* **2013**, *53*, 15.5.1–15.5.15.
- (52) Sofia, M. J.; Bao, D.; Chang, W.; Du, J.; Nagarathnam, D.; Rachakonda, S.; Reddy, P. G.; Ross, B. S.; Wang, P.; Zhang, H. R.; Bansal, S.; Espiritu, C.; Keilman, M.; Lam, A. M.; Steuer, H. M.; Niu, C.; Otto, M. J.; Furman, P. A. Discovery of a  $\beta$ -D-2′-Deoxy-2′- $\alpha$ -Fluoro-2′- $\beta$ -C-Methyluridine Nucleotide Prodrug (PSI-7977) for the Treatment of Hepatitis C Virus. *J. Med. Chem.* **2010**, *53*, 7202–7218.
- (53) Chapman, H.; Kernan, M.; Rohloff, J.; Sparacino, M.; Terhorst, T.; et al. Practical synthesis, separation, and stereochemical assignment of the PMPA pro-drug GS-7340. *Nucleosides, Nucleotides Nucleic Acids* **2001**, *20*, 1085–1090.
- (54) Cho, A.; Zhang, L.; Xu, J.; Lee, R.; Butler, T.; Metobo, S.; Aktoudianakis, V.; Lew, W.; Ye, H.; Clarke, M.; Doerffler, E.; Byun, D.; Wang, T.; Babusis, D.; Carey, A. C.; German, P.; Sauer, D.; Zhong, W.; Rossi, S.; Fenaux, M.; McHutchison, J. G.; Perry, J.; Feng, J.; Ray, A. S.; Kim, C. U. Discovery of the First C-Nucleoside HCV Polymerase Inhibitor (GS-6620) with Demonstrated Antiviral Response in HCV Infected Patients. *J. Med. Chem.* **2014**, *57*, 1812–1825.
- (55) Siccardi, D.; Kandalafi, L. E.; Gumbleton, M.; McGuigan, C. Stereoselective and concentration-dependent polarized epithelial permeability of a series of phosphoramidate triester prodrugs of d4T: an in vitro study in Caco-2 and Madin-Darby canine kidney cell monolayers. *J. Pharmacol. Exp. Ther.* **2003**, *307*, 1112–1119.
- (56) Allender, C. J.; Brain, K. R.; Ballatore, C.; Cahard, D.; Siddiqui, A.; McGuigan, C. Separation of individual antiviral nucleotide prodrugs from synthetic mixtures using cross-reactivity of a molecularly imprinted stationary phase. *Anal. Chim. Acta* **2001**, *435*, 107–113.
- (57) Mesplet, N.; Saito, Y.; Morin, P.; Agrofoglio, L. A. Liquid chromatographic separation of phosphoramidate diastereomers on a polysaccharide-type chiral stationary phase. *J. Chromatogr. A* **2003**, *983*, 115–124.
- (58) Ross, B. S.; Ganapati Reddy, P.; Zhang, H.-R.; Rachakonda, S.; Sofia, M. J. Synthesis of Diastereomerically Pure Nucleotide Phosphoramidates. *J. Org. Chem.* **2011**, *76*, 8311–8319.
- (59) Pertusati, F.; McGuigan, C. Diastereoselective synthesis of P-chirogenic phosphoramidate prodrugs of nucleoside analogues (ProTides) via copper catalysed reaction. *Chem. Commun.* **2015**, *51*, 8070–8073.
- (60) Arbelo Román, C.; Wasserthal, P.; Balzarini, J.; Meier, C. Diastereoselective Synthesis of (Aryloxy)phosphoramidate Prodrugs. *Eur. J. Org. Chem.* **2011**, *2011*, 4899–4909.
- (61) DiRocco, D. A.; Ji, Y.; Sherer, E. C.; Klapars, A.; Reibarkh, M.; Dropinski, J. J.; Mathew, R.; Maligres, P.; Hyde Alan, M.; Limanto, J.; Brunskill, A.; Ruck, R. T.; Campeau, L.-C.; Davies, I. W. A multifunctional catalyst that stereoselectively assembles prodrugs. *Science* **2017**, *356*, 426–430.
- (62) Slusarczyk, M.; Serpi, M.; Ghazaly, E.; Kariuki, B. M.; McGuigan, C.; Pepper, C. Single Diastereomers of the Clinical Anticancer ProTide Agents NUC-1031 and NUC-3373 Preferentially Target Cancer Stem Cells *In Vitro*. *J. Med. Chem.* **2021**, *64*, 8179–8193.
- (63) Slusarczyk, M.; Ferrari, V.; Serpi, M.; Gönczy, B.; Balzarini, J.; McGuigan, C. Symmetrical Diamidates as a Class of Phosphate Prodrugs to Deliver the 5′-Monophosphate Forms of Anticancer Nucleoside Analogues. *Chem. Med. Chem.* **2018**, *13*, 2305–2316.
- (64) McGuigan, C.; Bourdin, C.; Derudas, M.; Hamon, N.; Hinsinger, K.; Kandil, S.; Madela, K.; Meneghesso, S.; Pertusati, F.; Serpi, M.; Slusarczyk, M.; Chamberlain, S.; Kolykhalov, A.; Vernachio, J.; Vanpouille, C.; Introini, A.; Margolis, L.; Balzarini, J. Design, synthesis and biological evaluation of phosphorodiamidate prodrugs of antiviral and anticancer nucleosides. *Eur. J. Med. Chem.* **2013**, *70*, 326–340.
- (65) Pertusati, F.; McGuigan, C.; Serpi, M. Symmetrical diamidate prodrugs of nucleotide analogues for drug delivery. *Curr. Protoc. Nucleic Acid Chem.* **2015**, *60*, 15.6.1–15.6.10.
- (66) Surburg, H.; Panten, J. *Common Fragrance and Flavor Materials: Preparation, Properties and Uses*. 6th ed. Hoboken, NJ, 2016.
- (67) Jordan, C. T.; Upchurch, D.; Szilvassy, S. J.; Guzman, M. L.; Howard, D. S.; Pettigrew, A. L.; Meyerrose, T.; Rossi, R.; Grimes, B.; Rizzieri, D. A.; Luger, S. M.; Phillips, G. L. The interleukin-3 receptor alpha chain is a unique marker for human acute myelogenous leukemia stem cells. *Leukemia* **2000**, *14*, 1777–1784.
- (68) Wang, D.; Zou, L.; Jin, Q.; Hou, J.; Ge, G.; Yang, L. Human carboxylesterases: a comprehensive review. *Acta Pharm. Sin. B* **2018**, *8*, 699–712.
- (69) Kaspar, F.; Giessmann, R. T.; Krausch, N.; Neubauer, P.; Wagner, A.; Gimpel, M. A UV/Vis Spectroscopy-Based Assay for Monitoring of Transformations Between Nucleosides and Nucleobases. *Methods Protoc.* **2019**, *2*, 60.
- (70) Bahar, F. G.; Ohura, K.; Ogihara, T.; Imai, T. Species difference of esterase expression and hydrolase activity in plasma. *J. Pharm. Sci.* **2012**, *101*, 3979.
- (71) McGuigan, C.; Gilles, A.; Madela, K.; Aljarah, M.; Holl, S.; Jones, S.; Vernachio, J.; Hutchins, J.; Ames, B.; Bryant, K. D.; Gorovits, E.; Ganguly, B.; Hunley, D.; Hall, A.; Kolykhalov, A.; Liu, Y.; Muhammad, J.; Raja, N.; Walters, R.; Wang, J.; Chamberlain, S.; Henson, G. Phosphoramidate ProTides of 2′-C-methylguanosine as highly potent inhibitors of hepatitis C virus. Study of their in vitro and in vivo properties. *J. Med. Chem.* **2010**, *53*, 4949–4957.
- (72) Derudas, M.; Carta, D.; Brancale, A.; Vanpouille, C.; Lisco, A.; Margolis, L.; Balzarini, J.; McGuigan, C. The application of phosphoramidate ProTide technology to acyclovir confers anti-HIV inhibition. *J. Med. Chem.* **2009**, *52*, 5520–5530.
- (73) Satoh, Y.; Kadota, Y.; Oheda, Y.; Kuwahara, J.; Aikawa, S.; Matsuzawa, F.; Doi, H.; Aoyagi, T.; Sakuraba, H.; Itoh, K. Microbial serine carboxypeptidase inhibitors—comparative analysis of actions on homologous enzymes derived from man, yeast and wheat. *J. Antibiot.* **2004**, *57*, 316–325.
- (74) Congiatu, C.; Brancale, A.; McGuigan, C. Molecular modelling studies on the binding of some protides to the putative human phosphoramidase Hint1. *Nucleosides, Nucleotides Nucleic Acids* **2007**, *26*, 1121–1124.